



Contents lists available at ScienceDirect

Quaternary International

journal homepage: www.elsevier.com/locate/quaint

Bridging prehistoric caves with buried landscapes in the Swabian Jura (southwestern Germany)



Alvise Barbieri ^{a, f, *}, Carsten Leven ^b, Michael B. Toffolo ^a, Gregory W.L. Hodgins ^c,
Claus-Joachim Kind ^d, Nicholas J. Conard ^{a, e, f}, Christopher E. Miller ^{e, f}

^a Institute for Archaeological Sciences, University of Tübingen, Germany

^b Center for Applied Geosciences, Hydrogeology, University of Tübingen, Germany

^c Accelerator Mass Spectrometry Laboratory, University of Arizona, USA

^d Regierungspräsidium Stuttgart, Landesamt für Denkmalpflege, Germany

^e Department of Early Prehistory and Quaternary Ecology, University of Tübingen, Germany

^f Senckenberg Centre for Human Evolution and Paleoenvironment, University of Tübingen, Germany

ARTICLE INFO

Article history:

Received 31 January 2017

Received in revised form

8 June 2017

Accepted 1 August 2017

Available online 5 August 2017

Keywords:

Swabian Jura

Last Glacial Maximum (LGM)

Cave erosion

Landscape development

Gravettian

Magdalenian

ABSTRACT

The Ach and Lone valleys of the Swabian Jura represent two key areas for the study of the dispersal of modern humans into central Europe, owing to the presence of numerous cave sites in the region that contain stratigraphic sequences spanning the Middle and Upper Paleolithic. However, despite the relatively complete sequences contained within these caves, previous studies hypothesize that phases of erosion have influenced the preservation of Upper Paleolithic deposits, particularly those dating to the Gravettian. Furthermore, these same studies suggest that during the Late Glacial and Holocene, colluvial sediments subsequently covered these unconformities. In this paper we present a dataset that helps us evaluate how geomorphological processes active at the regional scale around the Last Glacial Maximum (LGM) have impacted the preservation of the archaeological record within the cave sites of the Ach and Lone valleys. To this end we applied and integrated a variety of methods, including geophysical prospecting, coring, micromorphology, Fourier Transform infrared (FTIR) spectroscopy, and radiocarbon dating. Our results show that alternating phases of soil formation, hillside denudation, river valley incision and floodplain aggradation have been the major processes active in Lone and Ach valleys throughout the Pleistocene and Holocene. These processes impacted the formation histories of the caves in the two valleys, thereby significantly influencing how we interpret the archaeological record of the region. In particular our data support the hypothesis arguing for the erosion of Gravettian-aged deposits (which are dated between 29,000 and 27,000 ¹⁴C BP) from the caves of Bockstein, Hohle Fels and possibly Hohlenstein-Stadel. Shortly after this erosive phase, increased depositional rates of loess nearly free of gravel and reworked soils marked in both the Ach and Lone valleys a shift towards colder and drier conditions corresponding with the LGM. Deteriorating climate likely forced Gravettian groups to abandon the Swabian Jura. The Magdalenian recolonization of the region took place in a cool interstadial (13,500–12,500 ¹⁴C BP) that was followed by a period of climate deterioration with minor phases of erosion in the caves and bedrock denudation. Towards the beginning of the Holocene the accumulation of frost debris (*Bergkies*) at the cave entrances marked the cessation of erosion within the caves.

© 2017 Elsevier Ltd and INQUA. All rights reserved.

1. Introduction

1.1. Linking caves with the landscape

Caves and rockshelters play a significant if outsized role in Paleolithic research. Humans preferentially selected these types of sites for habitation since the lower Paleolithic (e.g., Wonderwerk Cave, South Africa. [Malan and Cooke, 1941](#); [Beaumont and Vogel,](#)

* Corresponding author. Present address: Rümelinstraße 23, Tübingen, 72070, Germany.

E-mail address: alvise.barbieri@uni-tuebingen.de (A. Barbieri).

2006; Chazan et al., 2008) and their rich assemblages of archaeological materials—often found within well-stratified and datable deposits—have attracted the attention of archaeologists since at least the 19th century. However, despite the importance of caves for Paleolithic humans (and the scientists who investigate them), much, if not most, of the daily lives of foragers was carried out in the open air, and not in the confines of a natural shelter. By only focusing on the archaeological record of caves and rockshelters, we run the risk of forming biased views of the activities and behaviors of Paleolithic humans. Archaeologists recognize this bias (Conard, 2001) and have addressed these concerns through a wide range of methodological approaches that provide a link between activities conducted in the open air and the material remains recovered from excavations in caves (Castel et al., 1998; Çep and Waiblinger, 2001; Faith, 2007; Niven, 2007; Saladié et al., 2011; Starkovich, 2014; Yeshurun et al., 2007). Geoarchaeologists who study Paleolithic cave sites have similar concerns about linking data collected within a cave to processes that occur outside of a cave. Since the late 1970s (Goldberg, 1979), numerous micromorphological investigations have shown that paleoenvironmental changes influence the formation of cave deposits (Courty and Vallverdu, 2001; Goldberg et al., 2015; Karkanis, 2010; Mentzer, 2011; Sherwood et al., 2004). However, it is not always possible to form a link between micromorphological observations made at the microscopic or site scale with specific environmental processes (Courty and Vallverdu, 2001). This problem is exacerbated by the fact that researchers working in caves and those working in the open air often make observations at different scales and with different techniques: cave geoarchaeologists rely on micromorphology and field observations made over tens of centimeters and meters; landscape geoarchaeologists and quaternary geoscientists often focus on observations made over tens of meters or kilometers and study geomorphic features such as loess sequences (e.g. Terhorst et al., 2014), lake deposits (e.g. Litt et al., 2001) and river terraces (e.g. Vanderberghe, 2015). As a result, research focusing on “inside” deposits and “outside” deposits is often designed to answer very different questions. Furthermore, bridging open air and cave sequences relies on the comparison of chronological datasets, which are not always comparable between inside and outside of a cave, or the identification of lithological or pedological markers (e.g. Karkanis et al., 2015; Pirson et al., 2012), which do not necessarily extend from the open air into a cave environment.

In this paper, we present a case study conducted in the Ach and Lone valleys of the Swabian Jura, southwestern Germany—a region rich in Paleolithic cave sites, dynamic landscapes and a long research tradition. Here we attempt to link a paleolandscape study with geoarchaeological analysis of cave sediments by applying macro- and microscopic methods to both “outside” and “inside” deposits. This holistic approach to paleolandscape reconstruction and site formation processes allows us to assess the role that past environments played on depositional and post-depositional processes in the caves. Furthermore, by placing these important cave sites within a paleolandscape context, we are able to determine how landscape change in the Swabian Jura influenced the archaeological record of the caves and how humans in the Pleistocene exploited these natural shelters.

1.2. Geographic setting, geology and geomorphology

The Swabian Jura (or *Schwäbische Alb*) is a karstic plateau (between 500 and 1500 m amsl) located in southwestern Germany and delimited by The Neckar Valley to the north, the Black Forest to the west, the Nördlinger Ries to the east and The Danube Valley to the south (Fig. 1). The predominant bedrock present in this area is composed of limestones, mudstones, marls and sandstones which

formed in the Jurassic period (Black, Brown and White Jura in Fig. 1. Geyer and Gwinner, 1991; Schall, 2002). Part of the Swabian bedrock is composed of molasse and volcanic rocks formed in the course of the Miocene (Geyer and Gwinner, 1991). Relicts of tertiary sediments are often found reworked within karst features and dry valleys. Among them, the Bohnert-Formation is composed of peatized, iron oxide/hydroxide concretions embedded in kaolinite clay, and well sorted, rounded quartz sand (Ufrecht, 2008).

The presence of silt-sized particles of quartz, micas, hornblende and epidote in Quaternary-aged sediments indicate that during the Pleistocene the Swabian Jura was covered with loess (Gwinner, 1989; Schall, 2002; Goldberg et al., 2003; Miller, 2015; Barbieri and Miller, in press). However *in situ* loess deposits are nearly absent in the Swabian Jura north from the Danube (Sauer et al., 2016). Schall (2002) hypothesized that this absence is likely due to the relatively weak aeolian sedimentation and the intensive hillside denudation which were active in this region during and after the Würm Glaciation. After reworking, the loess of Swabia has been also affected by intensive diagenesis (Riek, 1957; Gwinner, 1989; Schall, 2002). In the study region, reworked but non-decalcified loess is commonly reported admixed with fine, elongated, platy, immature limestone gravel. This sediment type is named *Bergkies* and has been correlated with the breakdown of exposed bedrock during the stadials of the Würm glaciation (Riek, 1957, 1973; Wolff, 1962; Campen, 1990; Freund, 1998). *Bergkies* has been documented as an infilling of dry valleys (Wolff, 1962), caves, rockshelters and *abris* (e.g. Riek, 1957, Riek, 1973; Kind, 1987; Campen, 1990; Freund, 1998). Although it presents a lithology similar to the French *Grèzes Litées* (Bertran et al., 1992, 1994; Ozouf et al., 1995), the term *Bergkies* seems to indicate a slightly different sediment type, being coarser (up to 20 mm, Wolff, 1962) and not always bedded (Wolff, 1962).

The Ach and Lone valleys have been considerably shaped by alluvial processes. Starting from the Miocene, the Lone headwaters have been captured by the progressive southward expansion of the Neckar (Schall, 2002; Strasser et al., 2009). This process led to the present-day configuration of these two river basins probably around the Mindel-Haslach Interglacial (Schall, 2002; Strasser et al., 2009). On the contrary the Ach Valley formed in the Early Pleistocene, when the Paleo-Danube flowed in the Jura plateau between Ulm and Schelklingen (Fig. 1, detail 1 and 2. Gwinner, 1989; Strasser et al., 2009). Probably after the Eemian, the Danube migrated southward, roughly in its present location. Since then, the Ach is drained by three smaller karstic rivers: the Schmiech, Ach and Blau (Gwinner, 1989; German et al., 1995). Alluvial processes shaped these two valleys also in more recently in the Pleistocene; these processes were likely more active during colder periods when the aggradation of permafrost favored the formation of surficial drainages (German et al., 1995). In both valleys phases of river valley incision and floodplain aggradation resulted in the formation of river terraces, which, however, have been poorly studied (Dongus, 1974; German et al., 1995).

1.3. The Swabian Paleolithic

The Swabian Jura has been a key region for the study of the Paleolithic for the past 150 years, beginning with the pioneering work of Oscar Friedrich Fraas, Robert Rudolf Schmidt and Gustav Riek in the 19th and early 20th century and continuing to today, with recent excavations at Hohle Fels, Hohlenstein, and other localities (Schmidt, 1912; Riek, 1934; Kind and Beutelspacher, 2010; Beutelspacher et al., 2011; Bolus and Conard, 2012; Conard et al., 2015).

Although the region is probably best known for its evidence of early music and figurative art dating to the Aurignacian, the

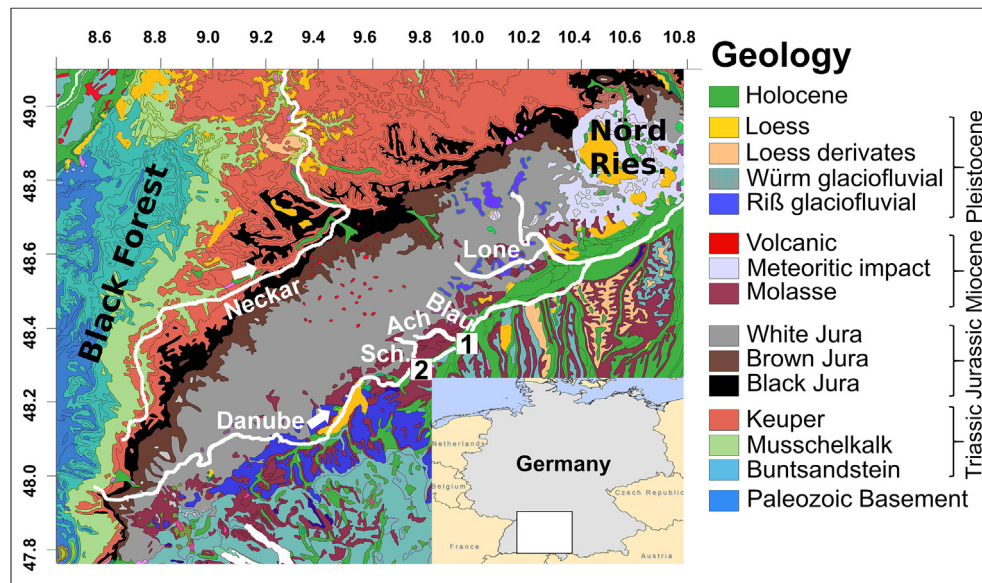


Fig. 1. Geological map of the Swabian Jura. 1, Ulm, 2, Schelklingen. Geological map compiled with data published in Geologische Karte Deutschland 1:1000000 (http://www.bgr.bund.de/EN/Home/homepage_node_en.html) and Sauer et al., 2016. The map is projected in the WGS 84 coordinate system. The labels along the upper and left axes indicate the WGS 84 coordinates.

Swabian Jura has also been a key area for investigating human settlement following the Last Glacial Maximum (Jochim et al., 1999; Kind, 2003; Teller, 2015). Upper Paleolithic sequences from southern Poland (Bobak et al., 2013), Switzerland (Leesch et al., 2012) and southwestern Germany (Conard and Bolus, 2003; Kind, 2003; Moreau, 2009) suggest that Magdalenian groups spread into central Europe after a period of depopulation coinciding with the LGM. Only southwestern France appears to have been continuously occupied during the Late Pleniglacial (Terberger, 2003). In Swabia Magdalenian recolonization took place in a short-lasting (13,500–12,500 ^{14}C BP, Kind, 2003, Teller, 2015) cool period characterized by grassland steppe with some forest biomes (Jahnke, 2013). Teller (2015) hypothesized that the climate amelioration of the Early Late Glacial might have affected hunting strategies and settlement dynamics of the Magdalenian groups, forcing them to leave Swabia.

1.4. The Paleolithic caves of the Ach and Lone valleys

Apart from a few notable exceptions (Bolus et al., 1999; Floss et al., 2012), almost all of the Paleolithic sites in Swabia are found in caves or rockshelters. For our study, we collected data from both the Ach and Lone valleys, but focused on linking our observations with three key cave sites: Hohlenstein and Bockstein in the Lone valley, and Hohle Fels in the Ach valley.

1.4.1. Hohlenstein

The name Hohlenstein indicates a limestone outcrop located in the Lone Valley (48.5495; 10.1725 WGS 84, Fig. 2), which hosts 4 distinct karstic cavities located approximately 3 m above the valley floor: Stadel, Bärenhöhle, Kleine Scheuer and Ostloch. Since the first excavation conducted by Oscar Fraas in the Bärenhöhle (Fraas, 1862), a number of researchers have investigated this karstic complex for over a century (Wetzel, 1961; Beck, 1999; Jahnke, 2013). In particular the cave of Hohlenstein-Stadel has gained much attention after the discovery of the Lion Man (*Löwenmensch*), which has been dated as one of the earliest examples of figurative art in Europe (Kind et al., 2014).

From 2008 to 2013 Claus-Joachim Kind and Thomas Beutelspacher have led the most recent excavations in this cave (Kind and Beutelspacher, 2010; Beutelspacher et al., 2011). During these years two distinct areas were investigated: at the back of the cave and at the entrance (area named *Vorplatz*, Fig. 3). Profiles exposed during these excavations have been sampled and analyzed with micromorphology (Barbieri and Miller, in press). Results from this analysis show that mass-wasting is the main process responsible for accumulation and erosion of sediment at this site. Sheet flow and gelifluction moved loess and other sediments originally deposited on top of the Jura into the karst system of Hohlenstein-Stadel (Fig. 4, detail 1). Here the originally calcareous loess underwent a process of phosphatization (Fig. 4, detail 2, Karkanias et al., 2002; Goldberg et al., 2003; Braillard et al., 2004; Shahack-Gross et al., 2004; Miller, 2015; Sanz et al., 2016; Barbieri and Miller, in press). This diagenetic process was not constant over time: the early Aurignacian deposits (Fig. 4, detail 3) display less intensive calcite dissolution and apatite neoformation. After undergoing phosphatization, cave sediments were periodically transported by sheet flow, mud flow and gelifluction from the back of Hohlenstein-Stadel towards the *Vorplatz* and the valley floor (Fig. 4, detail 5). Barbieri and Miller (in press) cite isolated grains of phosphatized loess in the otherwise non-phosphatized deposits of the *Vorplatz* (Fig. 4, detail 6) as evidence for this model. Cave erosion was more intensive probably around the LGM, when Gravettian-aged deposits were completely removed from Hohlenstein (Jahnke, 2013). After the LGM, mass-wasting originating from the cave redeposited Aurignacian artifacts at the cave entrance (unit GKS-2 in Fig. 4), on top of sediment yielding LGM to Late Glacial ^{14}C ages (unit KKS in Fig. 4, Jahnke, 2013). Later, cave erosion was much less intensive as suggested by the absence of grains of phosphatized loess in unit GKS-1 (Fig. 4). However, erosive processes might have lasted longer at the *Vorplatz*, where part of the Magdalenian deposit (unit GL2B, Fig. 4) has been removed (Jahnke, 2013). On top of this unconformity the deposition of unit GL2A marks a shift in sediment source with fresh loess and gravel moving from the hillside towards the cave entrance (Fig. 4).

In 1997 Schneidermeier (1999) investigated the hillside area

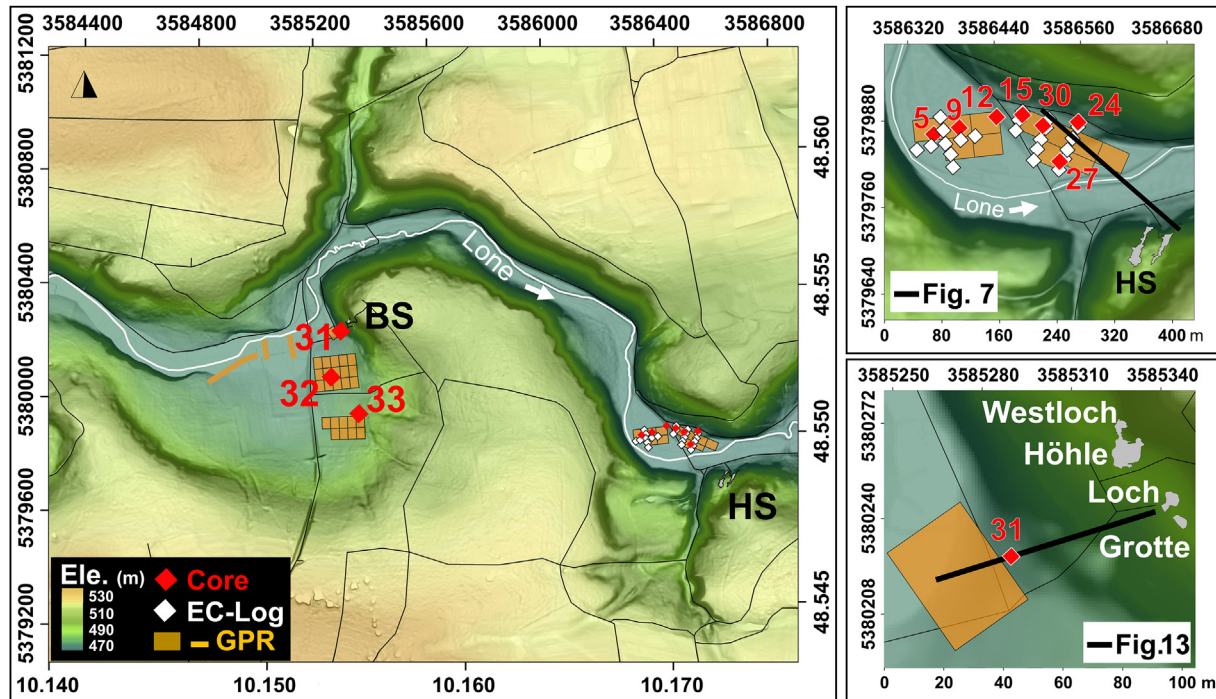


Fig. 2. Hohlenstein and Bockstein. *On the left*, geographic map showing the areas we surveyed in front of the cave complex of Bockstein and Hohlenstein. The map is compiled from Lidar data with 1 m resolution and it is projected in the DHDN Gauss-Krüger coordinate system. The labels along the upper and left axes indicate the DHDN Gauss-Krüger coordinates. The labels along the lower and right axes indicate the corresponding WGS 84 coordinates, which can be used to locate this map in Fig. 1. *On the upper right*, detail from the main map displaying the cores, ec-logs, and GPR grids we collected opposite from Hohlenstein. Cores are numbered in red. The black line indicates the position of Fig. 7. *On the lower right*, detail from the main map depicting the Bockstein cave complex, core 31 and the close by GPR grid. The black line indicates the location of Fig. 13. (For interpretation of the references to colour in this figure legend, the reader is referred to the web version of this article.)

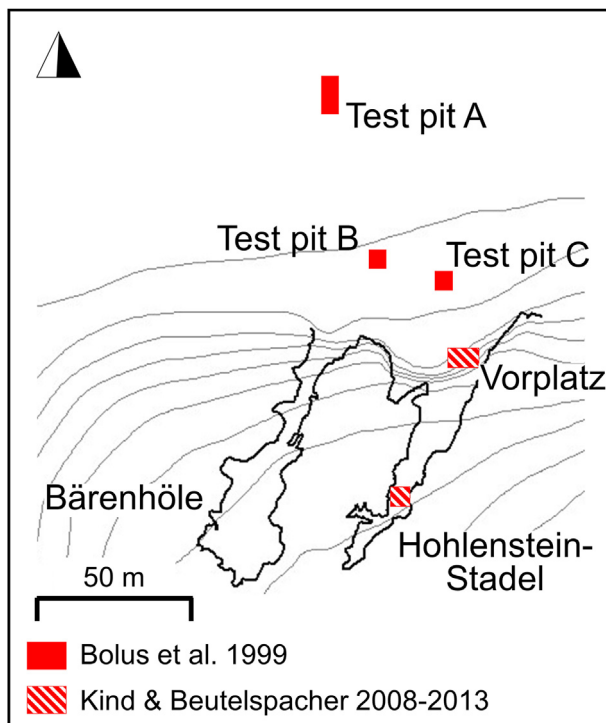


Fig. 3. Excavations at Hohlenstein. The location of the most recent archaeological excavations conducted inside and outside Hohlenstein-Stadel. Excavations conducted by Kind and Beutelspacher in the years 2008–2013 are marked with squares filled with red, diagonal dashes. Excavations conducted by Bolus et al. (1999) are marked with completely filled, red squares. (For interpretation of the references to colour in this figure legend, the reader is referred to the web version of this article.)

downslope from Hohlenstein. In his cores Schneidermeier (1999) recovered bone and stone tools. Based on his data a team of excavators led by Michael Bolus opened three small open-air test pits along the slope in front of the site (Bolus et al., 1999, Fig. 3). Two archaeological horizons were exposed during these excavations. Bolus (et al., 1999) and Geiling (et al., 2015) interpreted the upper GE1 horizon as mixed Holocene sediment of colluvial origin, while they considered the lower GE2 as a possibly less-disturbed Middle Paleolithic deposit containing 25 stone tools. However, Kitagawa (2014) suggested that the high amount of cave bear bones free from cut marks in GE2 might indicate that these materials originated from the Hohlenstein caves and were redeposited by mass-wasting processes.

1.4.2. Bockstein

The outcrop of Bockstein is located only a couple of kilometers westwards from Hohlenstein, in the Lone Valley (Fig. 2). Here, approximately 20 m above the floodplain, karstic processes have formed 4 small cavities, namely Bocksteinhöhle, Bockstein-Westloch, Bocksteingrotte and Bocksteinloch. Ludwig Bürger was the first to investigate this cave complex in 1879 (Krönneck, 2012) and between the 1930s and 1960s systematic archaeological excavations were carried under the direction of Robert Wetzel (Wetzel and Bosinski, 1969). During these three decades, the team lead by Wetzel removed almost all of the archaeological deposits accumulated inside the Bockstein caves and dug long trenches from Bocksteinhöhle and Bocksteinloch down to the Lone floodplain.

More recently, ^{14}C measurements (Conard and Bolus, 2003) and a re-evaluation of lithic assemblages (Borges de Magalhães, 2000) have been carried out on materials recovered from Bockstein-Törl.

This small cave presents a Middle Paleolithic sequence covered with a thinner deposit (BT VII) that contains a mixture of

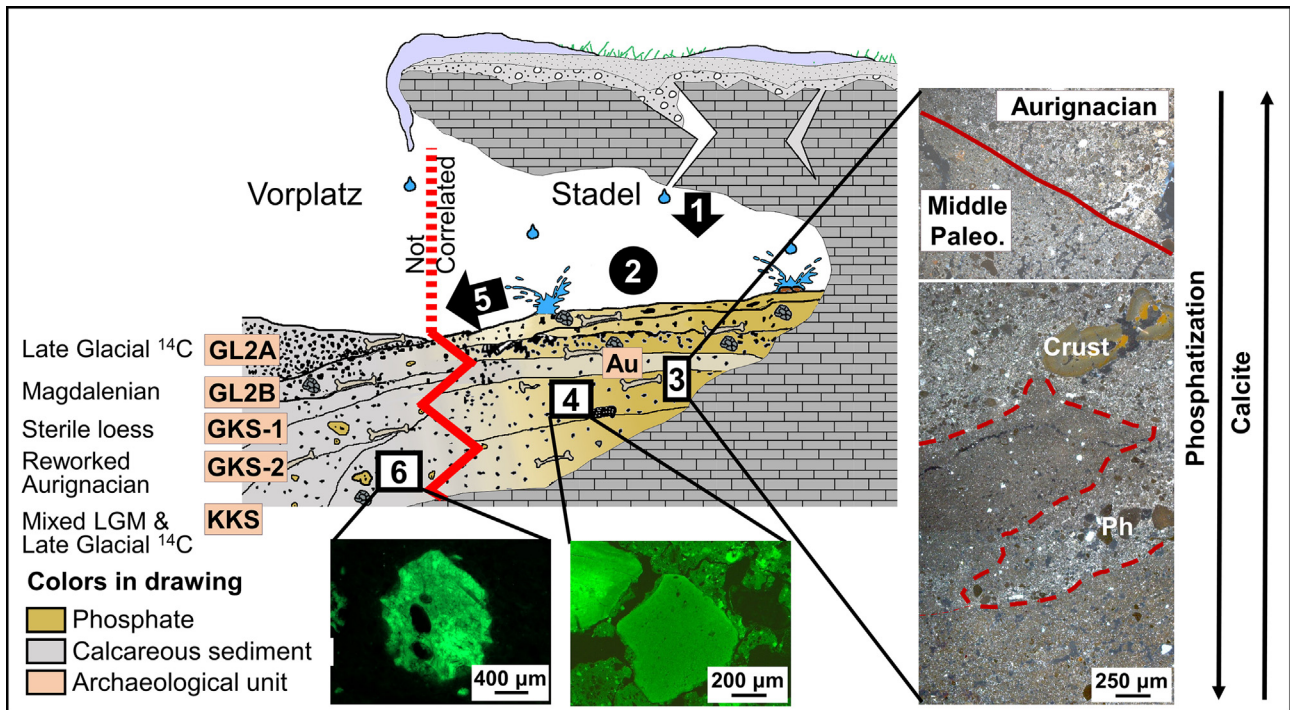


Fig. 4. Site formation processes at Hohlenstein-Stadel and Vorplatz. Idealized drawing of the sequence exposed by the archaeologists at the Vorplatz and at the back of the cave. The two excavations profiles are not correlated. In the drawing phosphatized sediment is depicted in light brown, while calcareous sediment is in gray. Archaeological units mentioned in the text are labelled in pink. Processes discussed in the text are depicted with numbers on black background: 1, sediment entered the cave through cracks, 2, sediments became phosphatized inside the cave, 5, sediment moved from the back of the cave towards the Vorplatz. Photomicrographs are labelled with connecting lines and numbers on white background: 3, photomicrographs collected in plain polarized light (here on PPL) at the contact between Early Aurignacian (Au) and Middle Paleolithic (Middle Paleo.) deposits preserved within Hohlenstein-Stadel. The Early Aurignacian deposit displays a better preservation of calcite (white speckles) and less intensive phosphatization in comparison with the Middle Paleolithic. Photomicrographs collected under fluorescent light (here on FL) of phosphatized loess in the back of the cave (4) and isolated grains of phosphatized loess in non-phosphatic sediment at the Vorplatz (6). (For interpretation of the references to colour in this figure legend, the reader is referred to the web version of this article.)

Aurignacian and Middle Paleolithic artifacts. The radiocarbon dating from this layer (from 46,000 BP to 30,000 BP) confirms its mixed nature (Conard and Bolus, 2003). On top of these sediments, three Gravettian deposits (BT VI-IV) have yielded dates from 31,500 BP to 20,000 BP (Conard and Bolus, 2003). Later infilling of Bockstein-Törle contains non-diagnostic Upper-Paleolithic stone tools and Neolithic artifacts.

Of particular interest for our research is the sequence that Wetzel exposed at the entrance of Bocksteinloch (the *Brandplatte* area), where he reported a deposit with mixed Upper and Middle Paleolithic stone tools of possible colluvial origin (Wetzel and Bosinski, 1969, p.18). Additionally, Schneidermeier (1999) investigated the Lone floodplain downhill from the Bockstein outcrop. His results confirm the general sedimentary sequence exposed by Wetzel along the hillside of Bockstein; however, Schneidermeier did not recover any artifacts in the river valley.

1.4.3. Hohle Fels

Hohle Fels is located approximately 3.5 m above the Ach floodplain, a few kilometers to the east of the town of Schelklingen (Fig. 5 detail 1). Archaeological excavations have been conducted at this site since the late 19th century, when Oscar Fraas and Theodor Hartmann recovered cave bear bones and artifacts shaped from stone, bone and antler (Hahn, 1978). Over the last two decades, seasonal excavation campaigns have been carried out by the University of Tübingen under the direction of Nicholas Conard and Maria Malina.

Previous geoarchaeological studies (Goldberg et al., 2003; Schiegl et al., 2003; Miller, 2015) have focused on the

micromorphological analysis of the Middle Paleolithic to Gravettian deposits accumulated inside the site. Results from these studies show that loess and soil material from the external hillside entered the cave through a large chimney located in the back of Hohle Fels. Once deposited inside this karstic cavity, sediments moved towards the cave entrance and underwent diagenesis similar to what Barbieri and Miller (in press) reported from Hohlenstein-Stadel. At Hohle Fels, Miller (2015) and Goldberg et al. (2003) emphasized the role of guano in the phosphatization processes. As observed at Hohlenstein-Stadel (Barbieri and Miller, in press.) and at the nearby site of Geißenklösterle (Miller, 2015, Fig. 5, detail 2), the replacement of calcite with apatite at Hohle Fels was less intensive in the early Aurignacian deposits. However, Late Aurignacian deposits display more intensive phosphatization, increased clay content and numerous clay infillings indicating wetter and warmer conditions. On top of these sediments the Gravettian-aged deposits display evidence of gelifluction, erosion and less intensive phosphatization (Miller, 2015; Goldberg et al., 2003). Recent archaeobotanical data from Hohle Fels published by Riehl et al., (2015) largely support the climatic fluctuations hypothesized by Miller (2015).

2. Methods

In this paper we present an innovative approach to landscape archaeology by integrating macro-, meso- and microscale techniques, including geophysical prospection, coring, lithostratigraphic description, Fourier Transform infrared (FTIR) spectroscopy, micromorphology and radiocarbon dating.

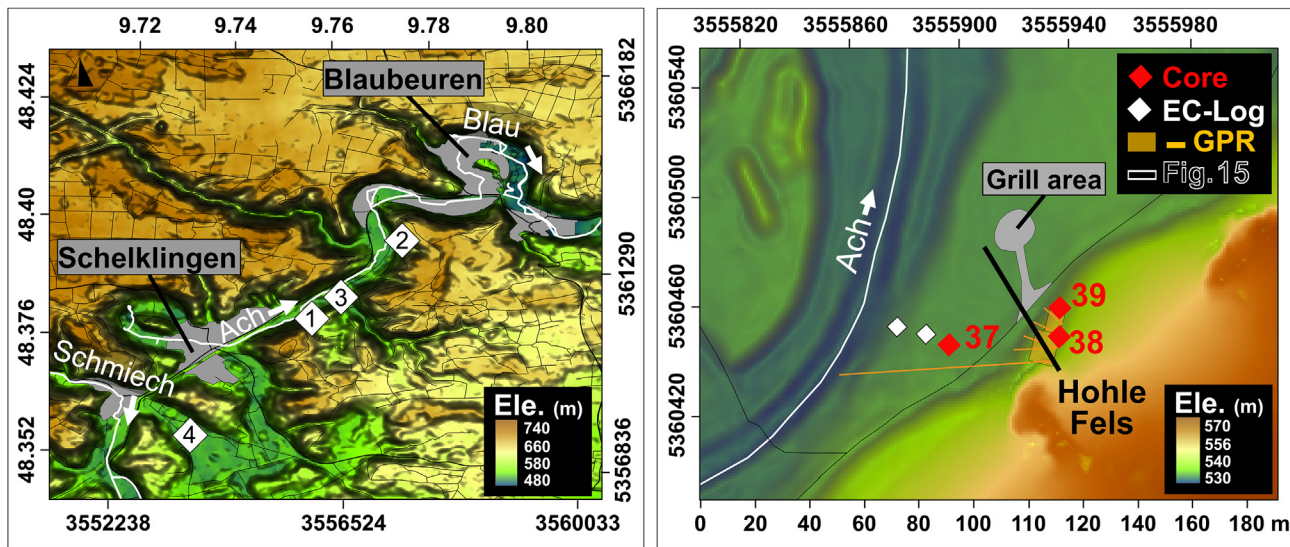


Fig. 5. Hohle Fels. **On the left**, geographic map displaying the location of: **1**, Hohle Fels; **2** Geißenklösterle; **3** core 7624/45 (Groschopf, 1973); **4** “Core Schmiecher See 1” (German et al., 1995). Towns are depicted in gray, rivers in white. The map is compiled from SRTM 90 m Digital Elevation Data and it is projected in the WGS 84 coordinate system. The labels along the upper and left axes indicate the WGS 84 coordinates, which can be used to locate this map in Fig. 1. The labels along the lower and right axes are the corresponding DHDN Gauss-Krüger coordinates, which can be used to locate the map depicted on the right. **On the right**, cores, ec-logs, and GPR measurements we collected in front of Hohle Fels. Cores are numbered in red. The black line indicates the position of Fig. 15. (For interpretation of the references to colour in this figure legend, the reader is referred to the web version of this article.)

2.1. GPR and EC-logging

We investigated depth-to-bedrock, grain size, structure and geometry of the deposits accumulated in the Ach and Lone valleys by applying Ground-Penetrating Radar (GPR) and Direct Push-based logging of electrical conductivity (EC). These techniques are complementary. GPR allows for the collection of continuous, high resolution, 2D-vertical time profiles of the shallow subsurface (Annan, 2009). On the other hand, EC-logging is used to acquire highly resolved, 1D-vertical depth profiles of electrical conductivity in unconsolidated sediments to a depth of 12 m (Leven et al., 2011). Therefore, EC-logging data do not necessitate post-collection processing (Schulmeister et al., 2003), can precisely deliver depth-to-bedrock and often facilitate the interpretation of geophysical measurements (e.g. Hoffmann et al., 2008).

In the course of the surveys we conducted in the Ach and Lone valleys we collected measurements in continuous mode (50–70 scans per meter) employing a GSSI TerraSIRch SIR System-3000 (SIR-3000) with a 200 MHz antenna (for details concerning the processing of the data, Supplementary 2: GPR data acquisition and processing). In the survey area nearby Hohlenstein and Hohle Fels, EC-logging was conducted using a Geoprobe® probing unit of the type 6610 DT in combination with a Direct Image® Soil Conductivity System of the type SC-500. During logging, direct current geoelectrical measurements are continuously applied with a four-pole downhole probe (diameter: 44.4 mm, distance between poles: 25.4 mm) using a Wenner array. Measurements are recorded every 1.5 cm. In the survey area nearby Hohlenstein, logging was performed down to bedrock, while in the area of Hohle Fels we proceeded down to a depth of 12 m. The position of the EC-logs was recorded in the field with D-GPS. With the software “R” we were able to associate geographic coordinates to each EC-log and export the result into a format compatible with GOCAD.

2.2. Coring

According to the information obtained from the geophysical

surveys, we focused our coring in a few key areas. Previous work (Schneidermeier, 1999) showed that the use of motor driven percussion coring devices were problematic in the recovery of sediments from the Lone Valley. This was likely a result of the high amount of gravel present in these sediments which frequently caused shallow refusal and sample mixing (Schneidermeier, 1999). To avoid similar issues, we used the same hydraulically-driven probing unit as employed for our EC-logging. The use of a Dual Tube Sampling System of the type DT325 guaranteed a good core recovery and penetration (average ca. 4 m, max 9.6 m) and prevented the possibility of sample mixing. We recovered almost all of our cores using this sampling system in 1.22 m long transparent polyethylene (PE) sample liners with a diameter of 50 mm. With the aim of reaching greater sampling depths, we recovered core 5 from the Hohlenstein area using a single-rod Geoprobe® Macro Core MC5 system. In this case sediment was recovered in 1.2 m long transparent PE liners with a diameter of 40 mm. All cores were recovered until bedrock was reached or probing refusal, and the geographic position of the coring locations were recorded with D-GPS.

At the end of the coring campaign we transported the cores to a facility of the Department of Geosciences in the city of Tübingen. Here we opened the liners and photographed, described and subsampled the recovered sediment. We distinguished over 300 geological layers (GL) based on their lithology. By comparing their lithology and stratigraphic position we subsequently grouped all the GL in 27 geological units (GU). As a final step, all of the data recovered from the cores was imported into GOCAD.

2.3. Micromorphology

In order to investigate depositional processes and sediment source, in addition to soil formation and post-depositional alteration, we sampled sediments recovered from the cores for micromorphological analysis. We collected 62 block samples focusing on the major geological units and their contacts. Blocks were extracted from the cores with the help of plaster bandages. We focused our

study on 26 of the most representative block samples. In the Geoarchaeology Laboratory of Tübingen we dried these blocks in the oven at ca. 40 °C for about 3 days. Afterwards, we impregnated them with a mixture of styrene, resin and hardener and let them consolidate for about three weeks in the fume hood. Once hardened we cut them with a rocksaw and ground them to a thickness of circa 30 µm. In total we produced 30 thin sections (6 × 9 cm) which we analyzed and described using petrographic microscopes in plane polarized (PPL), crossed polarized (XPL) and fluorescent light (FL) following terminology and protocols developed by [Stoops \(2003\)](#).

During the description of the thin sections we observed a few microstructural effects from the coring, in particular we noted a reduction in porosity and deformation of the original sedimentary structures along the sides of the samples. These effects were generally minor and obvious, and therefore did not significantly hinder the analysis.

2.4. Dating

We chose to date our sediments by ¹⁴C measurements rather than luminescence methods since we did not have the possibility to study and sample our cores under subdued, red or orange light. We were also encouraged to take advantage of radiocarbon dating given the large ¹⁴C dataset published for the Swabian caves by [Conard and Bolus \(2003, 2008\)](#). During the course of studying the recovered cores, we identified several materials that were potentially suitable for ¹⁴C dating, including possible fragments of charcoal and bone. We removed these materials from the cores and analyzed them using FTIR. A few milligrams of sample were homogenized and powdered in an agate mortar and pestle. About 0.1 mg were left in the mortar and mixed with approximately 0.5 mg of KBr (FT-IR grade, Sigma-Aldrich) and pressed into a 7-mm pellet using a hand press (PIKE Technologies). Infrared spectra were obtained at 4 cm⁻¹ resolution in 32 scans within the 4000–400 cm⁻¹ spectral range using an Agilent Technologies Cary 660 spectrometer. Phase identification was performed using Resolutions Pro, standard literature ([Van der Marel and Beutelspacher, 1976](#); [Lin-Vien et al., 1991](#)), and our in-house reference spectral library. The crystallinity index, or splitting factor, of carbonate hydroxyl-apatite (bone mineral) was calculated using the method of [Weiner and Bar-Yosef \(1990\)](#).

Based on the results of this analysis ([Supplementary 3: FTIR results](#)) we selected 7 samples for radiocarbon dating ([Table 1A](#) and [B](#)): three samples contained sufficient amounts of organic carbon (ID-19, ID-58 and ID-72), two samples were of gastropod shell fragments that displayed good preservation of aragonite (ID-69 and ID-73), one sample was of charcoal fragments (ID-57) and one sample was a bone fragment with a high degree of collagen preservation (ID-63). All of these samples were shipped to the AMS Laboratory at the University of Arizona in Tucson where they were pretreated and their ¹⁴C content measured.

Table 1A

Results of ¹⁴C measurements – **Part 1. ID**, sample name used in the text; **Lab number**, sample name used in the course of the analysis; **Core, GU** and **Depth** (below ground surface) indicate the location of the samples. **Material**, the type of specimen, **Pre-treat.**, process followed for pre-treatment, **Sample (mg)**, analyzed mass, **C (mg)**, mass of the extracted Carbon.

ID	Lab number	Core	GU	Depth (m)	Material	Pre-treat.	Sample (mg)	C (mg)
19	X29378	12	HS-GU4	-4.2	Tot. O. Carbon	A	518.48	0.47
57	X29380	37	HF-GU6	-1.2	Charcoal	A-B-A	3.79	2.52
58	X29381LT	37	HF-GU6	-1.5	Humins fraction	A	35.08	1.07
63	X29273	37	HF-GU3	-8.2	Bone	A-B-A	3.23	1.02
69	X29382	31	BS-GU3	-2.2	Aragonite shells	Etching	12.28	1.47
73	X29384	31	BS-GU3	-3.2	Aragonite shells	None	7.9	0.93
72	X29383LT	31	BS-GU2	-5.6	Tot. O. Carbon	A	649.27	1.44

The samples we selected for ¹⁴C dating were processed following different protocols. ID-19 and ID-72 were composed of reworked loess which we recovered from deeper than 4 m in core 12 and 31. Macroscopically these sediment did not display any organic matter, so we pretreated them with 1 N HCl acid in order to remove exclusively inorganic carbon and acid soluble organic molecules. ID-58 was composed of a peat-like sediment which was recovered in core 37 less than 2 m below the ground surface. With the aim of removing the younger carbon possibly translocated from overlying Holocene soils, we cleaned this sample with 1 N HCl acid, 0.1% NaOH followed by a final reacidification with HCl (so called acid-base-acid, ABA pretreatment. [Hatté et al., 2001](#); [McGeehin et al., 2001](#); [Pessenda et al., 2001](#); [Jull et al., 2013](#)). ID-19, ID-58 and ID-72 were collected from geological layers of colluvial origin (see the section below). By burning these samples at 400 °C we aimed at extracting the organic carbon that they might have incorporated around the time of their final burial ([McGeehin et al., 2001](#); [Wang et al., 2013](#)).

Charcoal and bone samples have been pretreated with ABA flow and burnt at high temperature (900–1100 °C). The two mixed shell samples (ID-69 and ID-73) were sonicated to remove any remaining sediment. Only ID-69 was large enough to be etched with a 100% H₃PO₄ solution to remove 50–85% of the carbonate, from both of them we have extracted carbon via hydrolysis using H₃PO₄ (as discussed by [Burr et al., 1992](#)).

The samples and their respective pretreatments are summarized in [Table 1A](#), dating results are listed in [Table 1B](#) (¹⁴C ages have been calibrated with the program OxCal 4.3 using the curve IntCal 13). All the dates mentioned in the text are ¹⁴C ages before calibration (¹⁴C BP).

3. Results

3.1. The Lone Valley in front of Hohlenstein

During the collection of pilot data in the Lone Valley, we

Table 1B

Results of ¹⁴C measurements – **Part 2. ID**, sample name used in the text; $\delta^{13}\text{C}(\pm 0.1\text{‰})$, measured $\delta^{13}\text{C}$; **¹⁴C age (¹⁴C BP)**, yielded ¹⁴C age; \pm , uncertainty of the ¹⁴C age; **Calibrate age 95%**, 2 σ calibration of the ¹⁴C age in calendar years Before/After Christ (**BCE/CE**) and Before Present (**BP**). ¹⁴C ages have been calibrated with the program OxCal 4.3 using the curve IntCal 13.

ID	$\delta^{13}\text{C} (\pm 0.1\text{‰})$	¹⁴ C age		Calibrate age 95%	
		(¹⁴ C BP)	\pm	(BCE/CE)	(BP)
19	-25.7	25,320	190	27,991–26,918 BCE	29,940–28,867
57	-26.9	314	40	1471–1651 AD	479–299
58	-28.5	4933	28	3771–3652 BCE	5720–5601
63	-21.6	27,900	460	31,102–29,107 BCE	33,051–31,056
69	-9.7	25,900	200	28,741–27,622 BCE	30,690–29,571
73	-7.3	28,280	270	31,029–29,497 BCE	32,978–31,446
72	-24.6	32,390	450	35,912–33,396 BCE	37,861–35,345

identified a break in slope located along the hillside opposite from the caves of Hohlenstein that, based on its morphology, strongly suggested the presence of a fluvial terrace (Fig. 2, detail on the upper right. Fig. 1, detail 1 in supplementary material). We decided to investigate this feature using GPR and covered this part of the slope and the downhill area of the Lone floodplain with 11 grids, each measuring 30×40 m. GPR profiles were measured with 1–3 m spacing along x and y grid axes. Based on the results of this survey we collected 7 cores (Supplementary 1.1: Hohlenstein) and 22 EC-logging profiles.

3.1.1. Depth-to-Bedrock

We used the depth of our EC-loggings to roughly reconstruct the bedrock topography. According to our data the White Jura limestone is located between 9.5 m and 2.8 m from the modern ground surface (Figs. 6 and 7). The bedrock appears deeper in the central part of the valley, where we detected a 100 m-large depression crossing our survey area from the northwest to the southeast. Our estimate of the bedrock depth and morphology is in agreement with the results of a seismic survey conducted by Schneidermeier (1999) on the opposite hillside.

3.1.2. HS-GU1 to HS-GU4

HS-GU1 rests on top of the bedrock and is composed of alternating silty clay and fine to coarse, subangular limestone gravel separated by sharp contacts (Fig. 6, HS-GU1, and Fig. 7, detail 1). Although we only recovered this unit in core 5, our EC-logging measurements revealed the presence of EC values comparable with HS-GU1 over an area of about 720 m². This deposit appears thicker along the hillsides (up to 3.5 m) and it gently (ca. 3°) dips towards the center of the valley, where it is no longer detectable (Fig. 7 supplementary material). The area in which we did not distinguish EC peaks comparable with HS-GU1 corresponds with the bedrock depression previously presented.

GL 315 is located towards the middle of HS-GU1 and displays a distinctive red color (7.5 R 4/6). Micromorphological results from this layer show that it is largely formed of aggregates of silt and clay

and iron-stained clay coatings exhibiting graded laminations. Clay coatings are dusty and laminated, even though boundaries separating the laminae are diffuse (Fig. 8, detail 1). Calcite is almost exclusively present in laminations of sand-sized grains (Fig. 8, detail 2).

We acquired EC-logging data below 6 m of depth. However, we were only able to recover sediment from below this depth in core 5; all other cores refused at this depth. Based on the EC-loggings and the refusal at depth, we hypothesize that in most of our boreholes the deeper HS-GU1 is covered with a deposit of coarser grained cobbles and likely boulders, a unit we designate as HS-GU2 (Fig. 6, HS-GU2, and Fig. 7, detail 2).

At the bottom of cores 5, 9, 12, 27 and 30 we recovered HS-GU3 (Fig. 6, HS-GU3, and Fig. 7, detail 3), which is composed of fine to medium, sub-rounded gravel of limestone, quartz and chert in a dark brown (10YR 3/3) silty sand composed of quartz and decalcified, reworked loess. In core 12 HS-GU3 appears laminated and poorer in gravel content. Our micromorphological results show that this unit is extensively impregnated with iron-manganese oxides and contains also fragments of laminated, limpid clay coatings (Fig. 8, detail 3). In comparison with HS-GU1, these fragmented coatings present more distinct laminae.

Above HS-GU3 we have distinguished HS-GU4 (Fig. 6, HS-GU4, and Fig. 7, detail 4), which is largely composed of decalcified, reworked loess and clay. Radiocarbon measurements on the total organic carbon from this unit has yielded an age of 25.320 ± 190 BP (Table 1B, ID-19). Our micromorphological results from this deposit revealed the presence of fragmented, laminated, limpid clay coatings similar to those described for HS-GU3. We have additionally observed typical, disorthic, iron-manganese nodules and aggregates composed of reworked loess and clay. These aggregates are composed of smaller angular pedes separated by star-shaped vughs which have been infilled with iron-manganese oxides. Occasionally these smaller pedes present pressure faces. Particularly in the area of the upper contact with HS-GU5, the groundmass of HS-GU4 appears formed of granular, densely-packed aggregates displaying granostriated b-fabric (Fig. 9, detail 1).

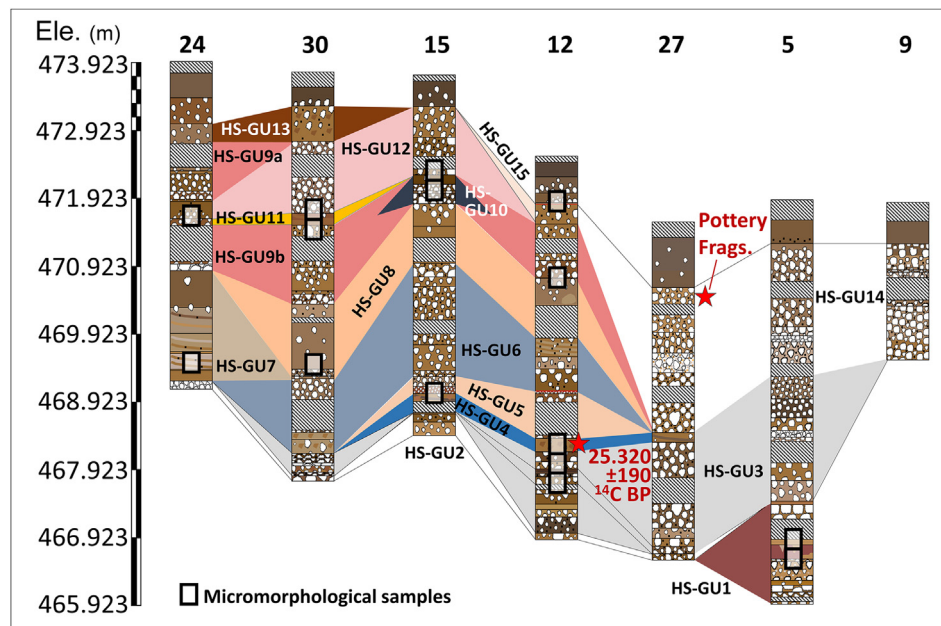


Fig. 6. Cross-correlation of the cores collected in front of Hohlenstein. White rectangles indicate the analyzed micromorphological samples, red stars mark the location of dating material. (For interpretation of the references to colour in this figure legend, the reader is referred to the web version of this article.)

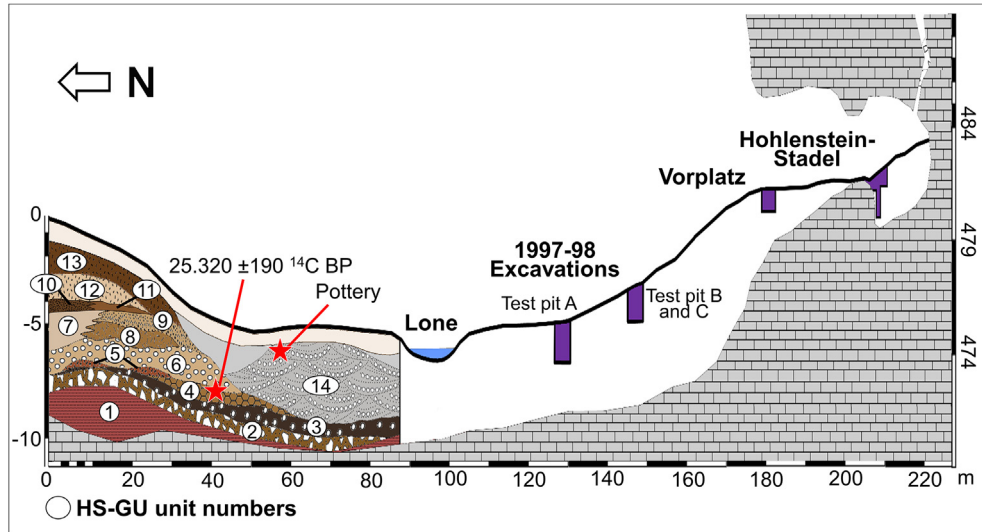


Fig. 7. Section across The Lone Valley in front of Hohlenstein. This figure is based on data from our geophysical measurements and coring, the location of this section is plotted in Fig. 2, upper right detail. HS-GUs are numbered on the profile.

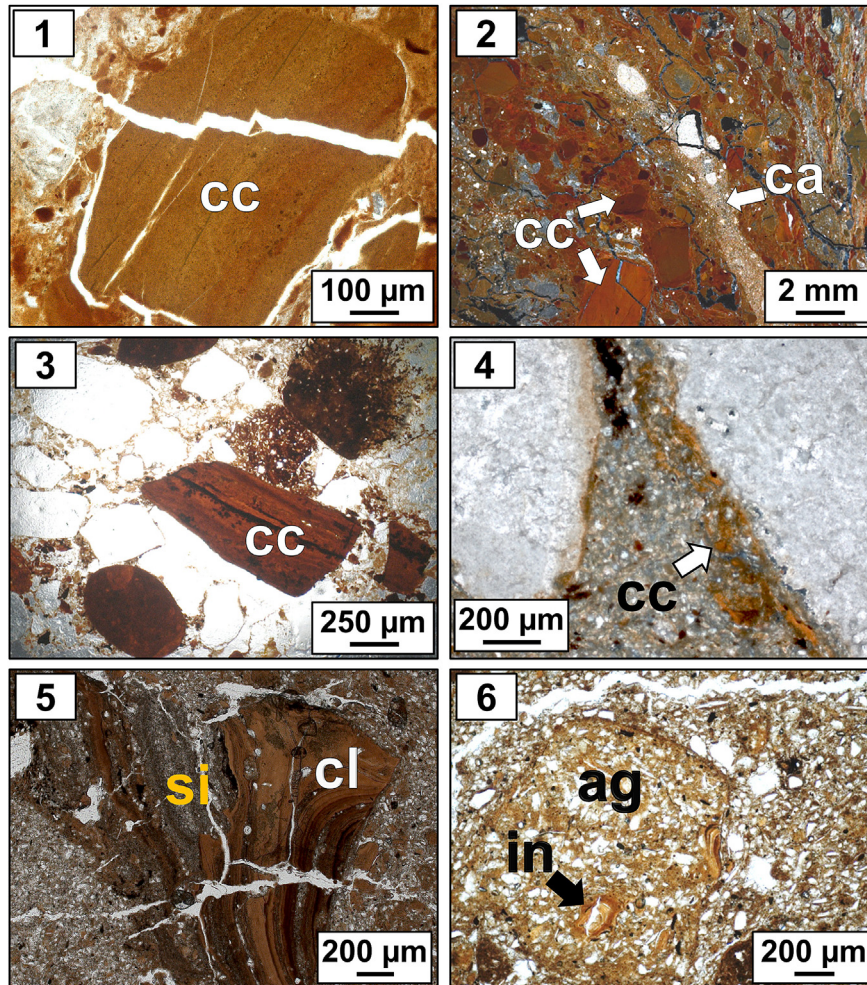


Fig. 8. Clay coatings from the area opposite from Hohlenstein. 1, photomicrograph in PPL of fragmented, dusty, iron stained clay coating (cc) exhibiting graded laminations, from HS-GU1. 2, photomicrograph in cross polarized light (here on XPL) depicting alternating laminations of calcite sand (ca) and fragmented, iron stained clay coatings (cc), from HS-GU1. 3, photomicrograph in PPL of fragmented, laminated, limpid clay coating, from HS-GU3. 4, photomicrograph in XPL of limpid clay coating (cc) displaced from the limestone gravel on which it originally formed, from HS-GU8. 5, photomicrograph in PPL of fragmented, layered coating displaying alternating laminations of silt (si) and clay (cl), from HS-GU10.6, photomicrograph in PPL of reworked clay aggregate (ag) displaying clay infillings (in), from HS-GU11.

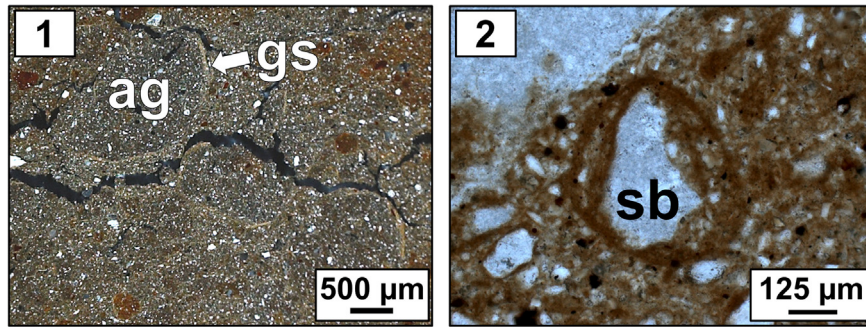


Fig. 9. Examples of potential cryogenic microfibrils from the area opposite from Hohlenstein. **1**, photomicrograph in XPL displaying well-rounded fine fraction aggregates (**ag**) delimited by granostriated b-fabric (**gs**), from the upper contact of HS-GU4. **2**, photomicrograph in PPL “snow ball” (Rose et al., 2000) (**sb**) composed of a medium sand-sized calcite grain coated with concentric and alternating laminations of silt and iron stained clay, from HS-GU5.

3.1.3. HS-GU5 to HS-GU13

On top of HS-GU4 we have documented two different sequences: HS-GU5 through HS-GU13 accumulated along the northern hillside of the valley and HS-GU14 accumulated exclusively in the center of the Lone flood plain (Figs. 6 and 7).

The sequence HS-GU5–13 is mainly composed of reworked loess and angular, fresh, occasionally platy limestone debris ranging from fine (Fig. 10) to coarse gravel-sized. These components are organized in beds that vary from matrix-to clast-supported. The color of the matrix alternates between reddish-brown and yellowish-brown. In thin section we observed reworked limpid clay coatings (Fig. 8, detail 4), fragmented compound-layered coatings composed of clay and silt (Fig. 8, detail 5), clay aggregates and *in situ* to reworked, dense, incomplete to complete clay infillings (Fig. 8, detail 6). In HS-GU5 we observed well-rounded aggregates composed of sand-sized fragments of calcite coated with alternating laminations of clay and silt (Fig. 9, detail 2).

HS-GU7 is unusual within the HS-GU5–13 sequence in that it is composed of laminated, reworked, and partly decalcified loess nearly free of limestone gravel and fragmented clay coatings (Fig. 6, HS-GU7, and Fig. 7, detail 7).

The presence of shallow units richer in silty clay (such as HS-GU7, HS-GU11 and HS-GU13) limited the penetration of our GPR measurements along the hillside. Only in the area between cores 15 and 30 could our geophysical data reveal clear structures (Fig. 5 in Supplementary material). In this part of the slope at a depth comparable with HS-GU12 we detected 10×5 m large reflectors densely stacked in an imbricated fashion (Blikra and Nemeč, 1998). At the passage between hillside and floodplain the GPR reflectors

corresponding to HS-GU12 and 11 appear truncated by other reflectors dipping towards the center of the plain with an angle of ca. 11° (Fig. 7, lower detail).

3.1.4. HS-GU14

Our coring and GPR data indicate that in the floodplain this disconformity has been covered with sediments much different from the HS-GU5–13 deposits (Fig. 6, HS-GU14, and Fig. 7, detail 14). In cores 5, 9 and 27 we recovered almost dry, well-rounded to angular, coarse, medium and fine gravel which we distinguished as HS-GU14. The gravel of this unit is largely composed of limestone fragments, while quartz, Bohnerz and chert are occasionally present. In the top part of this unit (core 27) we found rare fragments of pottery (2–4 mm).

Our GPR results from the floodplain show the presence of laterally continuous reflectors (2×2 m to 5×5 m) that are located at depths between -1 m and -3 m and dip (3° – 5°) northwards, towards the hillside (Fig. 11, detail A). In the passage between hillside and floodplain these potential beds appear truncated by a nearly continuous reflector that appears to delineate a 1 m deep, ca. 10 m wide and 80 m long depression (Fig. 11, detail B). Velocity analysis of the GPR measurements (Davids and Annan, 1989) and additional augering revealed that this depression is filled with silty clay sediments. On the southernmost edge of our survey area, we have detected other laterally continuous reflectors (up to 10×30 m

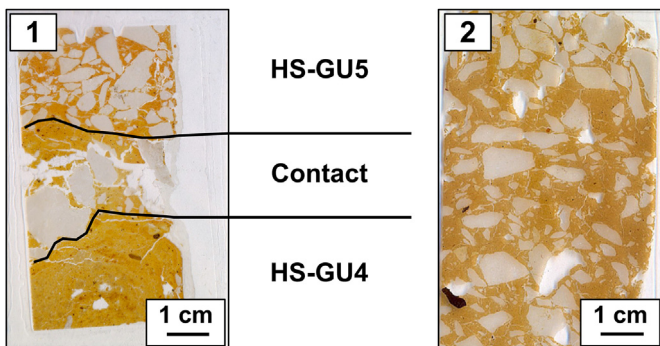


Fig. 10. Examples of Bergkies from the area opposite from Hohlenstein. **1**, thin section scan depicting the contact between HS-GU4 and HS-GU5. To be noted the fine limestone gravel (Bergkies) of HS-GU5. **2**, thin section scan depicting the fine, poorly laminated gravel (Bergkies) of HS-GU11.

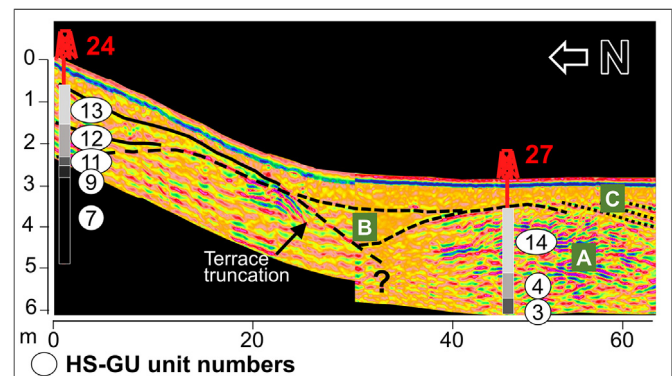


Fig. 11. Terrace truncation from the area opposite from Hohlenstein. Two merged GPR profiles from core 24 to core 27 (numbered in red) which display reflectors likely indicative for an incision of the HS-GU5–11 sequence accumulated along the hillside (Terrace truncation). **A**, gravelly deposits resulting from northwards migrations of the Lone. **B**, potential channel filled with silty clay sediments. **C**, sedimentary structures suggesting a final southwards migration of a paleo-channel. (For interpretation of the references to colour in this figure legend, the reader is referred to the web version of this article.)

large) that dip (3°) towards the south, in the direction of the Lone River (Fig. 11, detail C).

3.2. The Lone Valley in front of Bockstein

Along the hillside and floodplain located downhill from the Bockstein caves we collected a GPR survey composed of 20 grids (30×40 m each, Fig. 2). Similar to the prospections conducted in the surroundings of Hohlenstein, GPR profiles were collected along the x and y axes of each grid with 1–2 m spacing. GPR data from the Bockstein area showed strong attenuation of the electromagnetic signal likely caused by higher silt content of the sediments located below the modern soil. Nevertheless, the GPR proved to be effective in detecting gravelly deposits that accumulated in a few discrete areas along the base of the hill. From these areas we collected three cores: 31, 32 and 33 (Supplementary 1.2: Bockstein). The sequence we recorded from core 31 is the most representative and is summarized below.

3.2.1. BS-GU2

At the bottom of core 31 we recovered well-rounded gravel alternating with beds composed of silt and rarer, angular gravel (Fig. 12, BS-GU2, and Fig. 13, detail 2). Both bed types are composed of fine to coarse limestone, Bohnerz and chert gravel. Among these sediments, GL 266 presents composition and color comparable with that described for HS-GU3. Our micromorphological analysis of GL 266 revealed the presence of fragmented, laminated, limpid clay coatings similar to those reported for HS-GU3 (Fig. 13, detail A), redeposited soil aggregates, in addition to disorthic and orthic iron-manganese nodules. We also identified small bone fragments (500 μm at maximum length, Fig. 13, detail B) and coarse gravel composed of chert. From the underlying GL 268 we conducted measurements on the total organic carbon, obtaining an age of 32.390 ± 450 ^{14}C BP (Table 1B, ID 72).

3.2.2. BS-GU3

In the central and lower part of core 31 we observed laminations of partly decalcified loess alternating with occasional beds of medium to fine, subrounded limestone gravel (Fig. 12, detail BS-GU3,

and Fig. 13, detail 3). In addition to loess, our micromorphological analysis revealed that BS-GU3 contains snail shells, rare fragments of limpid clay coatings and bones (up to 250 μm maximum length). We also identified aggregates composed of rare silt-sized grains of quartz and mica embedded within a phosphatic groundmass, which we interpreted as phosphatized grains of loess (Goldberg et al., 2003; Miller, 2015; Barbieri and Miller, in press, Fig. 13, detail C). We performed radiocarbon measurements on the aragonite from two assemblages of snail shell fragments, collected at 4 m and 2 m below the ground surface. The deeper sample has been dated at 28.280 ± 270 ^{14}C BP (Table 1B, ID 73), while the shallower has yielded a date of 25.900 ± 200 ^{14}C BP (Table 1B, ID 69).

3.2.3. BS-GU4

In terms of composition, BS-GU3 presents substantial similarities with the overlying BS-GU4 (Fig. 12, BS-GU4, and Fig. 13, detail 4). The main difference is represented by the upward increase in mean grain size and gravel content. In BS-GU4 fragments of bone and phosphatized grains of loess are even more abundant than below and appear larger in size (500 μm maximum length, Fig. 13, detail D).

3.2.4. BS-GU5

From the uppermost part of core 31 we observed open, loose, angular limestone gravel (Fig. 12, BS-GU5). Given the loose nature of this deposit we have not investigated it with micromorphological analysis. Our GPR data show that BS-GU5 presents slightly imbricated bedding (Blikra and Nemeč, 1998) comparable with HS-GU12 (Fig. 13, detail 5). Furthermore, the GPR data suggests that this unit is not laterally continuous and possibly covers a silty deposit that was not recovered within core 31 (silty clay in Fig. 13).

3.3. The Ach valley in front of Hohle Fels

Here we focused our surveys on the break-in-slope (Vorplatz) and the flood plain area located directly in front of the entrance to Hohle Fels cave (Fig. 5, detail on the right). We covered the Vorplatz with two smaller grids, respectively 9×12 m and 6×8 m. In each grid we measured GPR profiles along the x and y axes with a spacing of 1 m. We collected additional, freely oriented lines around the Hohle Fels area and along the Ach plain. Based on our GPR results we recovered 2 cores from the Vorplatz and 1 core and 2 EC-logging profiles from the floodplain (Also Supplementary 1.3: Hohle Fels).

3.3.1. HF-GU1

In this GU we have grouped all the units recovered within core 38 and 39 from the Vorplatz area (Fig. 14, HF-GU1). These sediments are composed of loose, angular, fine to coarse limestone gravel alternating with non-decalcified, reworked loess.

At the Vorplatz the maximum depth reached with both our GPR and coring data was about 5 m. Further penetration was likely impeded by an aquifer that we encountered in core 38 at 4.8 m below the ground surface (Fig. 15, detail A). Our attempt to recover sediments buried below this depth was unsuccessful, due to the water saturation of these deposits.

Moving from core 38 towards core 39 the GPR signal attenuated also at shallower depth (Fig. 15, detail A). Sediments recovered from this latter core display a higher content of silty clay in comparison with those contained within core 38 (Fig. 14). This difference in grain size has probably led to a more intensive upwards capillary movement of ground water from the water table in this part of the Vorplatz (Lu and Sato, 2007).

At about 4 m below the surface we identified a reflector that dips gently from the Hohle Fels cave entrance towards the center of

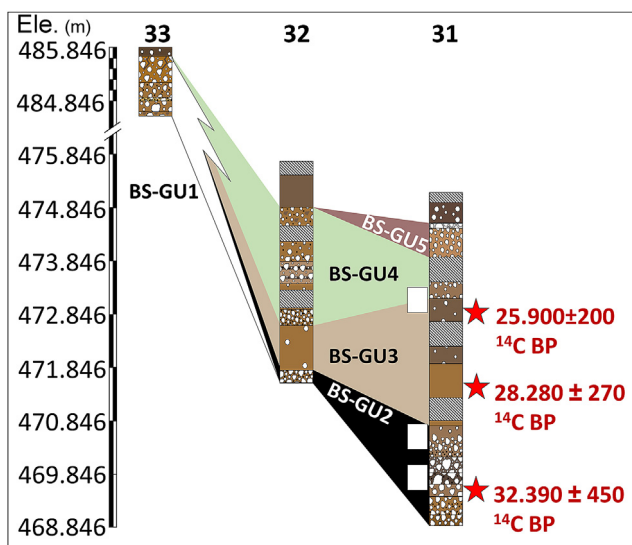


Fig. 12. Cross-correlation of the cores collected in front of Bockstein. White rectangles indicate the analyzed micromorphological samples, red stars mark the location of dating material. (For interpretation of the references to colour in this figure legend, the reader is referred to the web version of this article.)

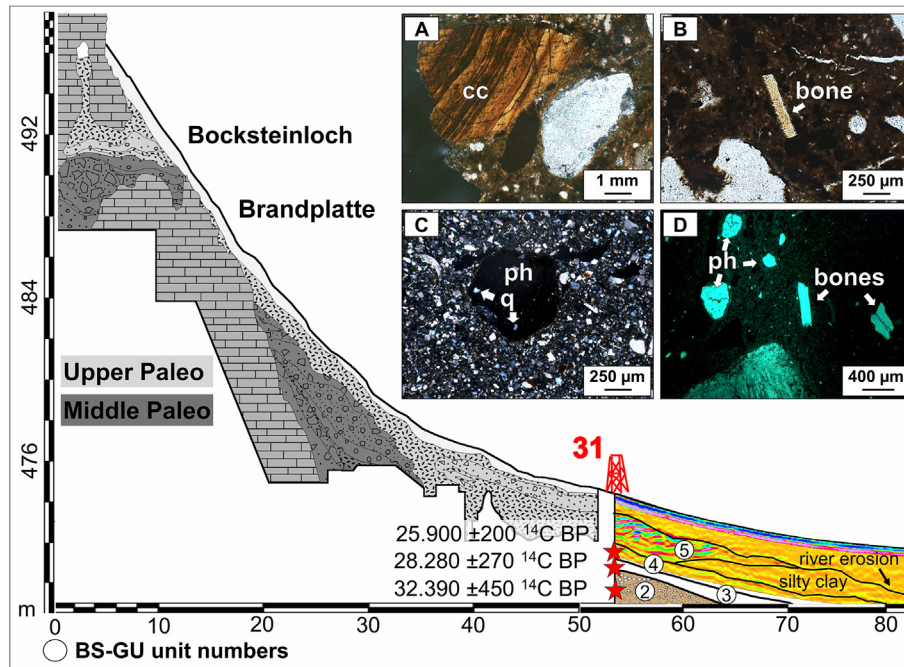


Fig. 13. Section from Bocksteinloch down to The Lone Valley. This figure is based on data published in this article and drawings of cross sections from the excavations conducted by Wetzel along the hillside (Wetzel, 1958). Location of this section is indicated in Fig. 2, lower right. The BS-GUs mentioned in the text are numbered on the GPR profile and on the drawing. In the GPR profile, the imbricated bedding of BS-GU5 (5) is comparable to HS-GU12 (see Fig. 5 in Supplementary material). **A.** photomicrograph in XPL of fragmented, limpid, laminated clay coating (cc), from BS-GU2. **B.** photomicrograph in PPL of bone fragment (bone), from BS-GU2. **C.** photomicrograph in XPL of isolated grain of phosphatized loess displaying rare silt-sized grains of quartz (q) embedded in a phosphatic groundmass (ph), from BS-GU3. **D.** photomicrograph in FL depicting isolated grains of phosphatized loess (ph) and bone fragments (bones), from BS-GU4.

The Ach Valley (Fig. 15, detail A.α). This feature corresponds to the lower part of core 38 and 39 from where we have also recovered sand-sized fragments of speleothems. Around 1–2 m below the surface we detected reflectors defining an irregular, 14 × 5 m large surface (Fig. 15, detail A.β). Above this discontinuity we have distinguished densely stacked reflectors which dip towards the Hohle Fels cave entrance and The Ach Valley (Fig. 15, detail A.γ). These sedimentary bodies appear truncated on top by the present day topography.

3.3.2. HF-GU2 to HF-GU4

HF-GU2–4 correspond to the lowermost deposits we have recovered from The Ach Valley (from –4.8 m to –9.6 m) and they are composed of angular to subrounded, fine to medium limestone gravel alternating with beds of decalcified, reworked loess (Fig. 14, HF-GU2, HF-GU3, HF-GU4. Fig. 15, detail 2, 3 and 4). Our micro-morphological analysis from the lower portion of HF-GU2 reveal the presence of sand-sized fragments of speleothem, phosphatized grains of loess, reworked limpid clay coatings (Fig. 15, detail B, C and D) and bone. Additionally, from the lower part of HF-GU3 we have recovered a larger bone fragment (about 2 cm²) that has yielded a radiocarbon age of 27,900 ± 460 ¹⁴C BP (Table 1 B, Fig. 15, detail E).

The gray color of the groundmass suggests that these sediments have been extensively gleyed (Lindbo et al., 2010).

3.3.3. HF-GU5

Stratigraphically above HF-GU4, HF-GU5 (Fig. 14, HF-GU5, and Fig. 15, detail 5) is composed of graded laminations and lenses of well-sorted, non-decalcified, coarse, reworked loess. In comparison to the lower units, HF-GU5 appears richer in iron oxide features.

3.3.4. HF-GU6

HF-GU6 is composed of decalcified and reworked loess, organic matter, rare sand-sized fragments of charcoal, and occasional sand-sized grains of pottery (Fig. 14, HF-GU6, and Fig. 15, detail 6). This deposit appears well-sorted and exhibits graded laminations. The contact with the lower HF-GU5 displays channels and bio-galleries in which we have observed fragments of laminated, limpid clay coatings and matrix aggregates moved from HF-GU6 downwards into HF-GU5.

From HF-GU6 we collected two samples for radiocarbon measurements. From the lower part of this unit a sample of the humin fraction has been dated to 4,933 ± 28 ¹⁴C BP (Table 1 B, ID 58); a few decimeters upwards a mixed sample of charcoal fragments has yielded an age of 314 ± 40 ¹⁴C BP (Table 1 B, ID 57).

3.3.5. HF-GU7

HF-GU7 is the uppermost unit we recovered from the flood plain (Fig. 14, HF-GU7, and Fig. 15, detail 7). It is composed of bedded limestone gravel displaying different degrees of roundness (from subangular to rounded) and size (from coarse to fine). We have also observed rare fragments of glazed pottery and Bohnerz.

4. Discussion

Our data collected in this study suggests that the landscape within both the Ach and Lone valleys has been variably shaped by phases of soil formation, soil denudation, loess accumulation and river incision. Below we provide a diachronic discussion of these processes as they relate to the areas around Hohlenstein, Bockstein and Hohle Fels. We then discuss what influence these processes had on the Paleolithic cave sites of the region.

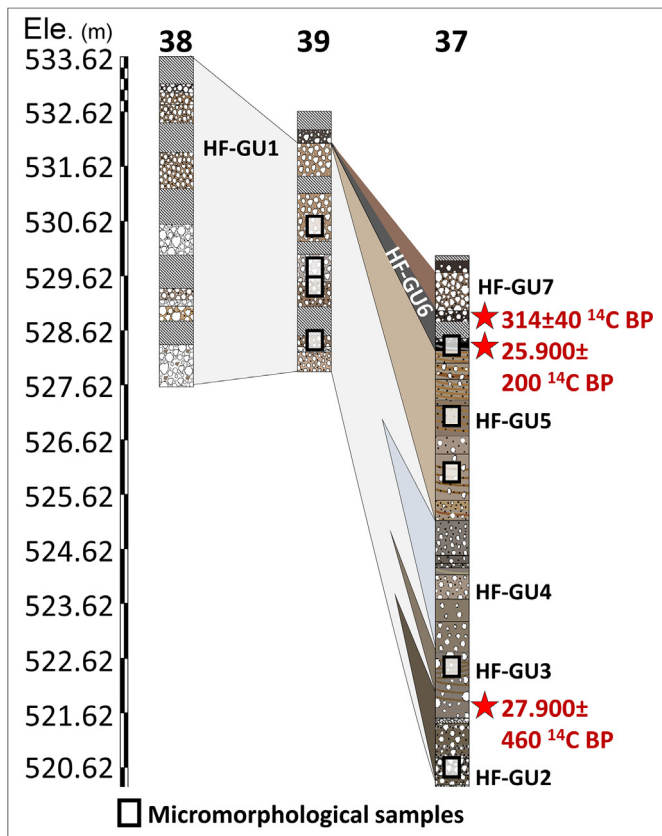


Fig. 14. Cross-correlation of the cores collected in front of Hohle Fels. White rectangles indicate the analyzed micromorphological samples, red stars mark the location of dating material. (For interpretation of the references to colour in this figure legend, the reader is referred to the web version of this article.)

4.1. Landscape formation processes in front of Hohlenstein in the Lone Valley

4.1.1. Soil formation, soil erosion, possibly river incision (pre-Quaternary and Pleistocene)

Given the subangular gravel and the sharp contacts we have described within HS-GU1, we hypothesize that this unit represents the earliest evidence for hillside erosion that we have recovered from the Lone Valley. Within it, GL 315 is largely formed of iron-stained clay, which has been redeposited as aggregates and fragments of dusty, laminated clay coatings organized in graded laminations (Fig. 8, detail 1 and 2). Therefore GL 315 might be regarded as a phase of soil re-deposition.

We suggest that the clay deposited in GL 315 originated from a soil that likely formed under a relatively warm and wet environment that promoted nearly complete dissolution of calcium carbonate, clay neoformation and subsequent clay illuviation. Later this soil was eroded and redeposited. Due to the lack of details concerning the geometry of GL 315 we are not able to clarify whether this layer has been deposited by surface runoff or channelized water (Blikra and Nemeč, 1998). Sediments similar to GL 315 have been described by Kösel (2016) at the near-by area of Hörvelsingen, from where he has reported a kaolinite- and hematite-rich sediment just below the Holocene soil. According to the hypothesis of Kösel (2016), this soil might have formed during an intensive weathering phase preceding the Quaternary. During the Pleistocene, the soil was likely eroded and redeposited by periglacial processes.

Our EC-logging data indicate that HS-GU1 may have been

eroded away from the central part of the Lone valley. Interestingly, the area in which we did not detect HS-GU1 coincides with a 100 m-large depression in the limestone bedrock, which crosses our survey area from the northwest to the southeast (Fig. 7 in this text and Fig. 7 in the supplementary material). Based on the morphology of HS-GU1 and the underlying bedrock, we hypothesize that the Lone River may have removed HS-GU1 from the central part of the valley and additionally carved the underlying limestone bedrock during a phase of river incision. Examining the difference between maximum elevation of HS-GU1 along the hill-sides and minimum elevation of the bedrock in the center of the Lone Valley we suggest that during this erosive phase the Lone might have lowered the valley floor by up to 3.5 m.

4.1.2. Soil formation, soil erosion, major loess deposition (around 25.000 ^{14}C BP)

In HS-GU3 and HS-GU4 we identified fragmented limpid clay coatings (Fig. 8, detail 3), reworked manganese nodules and reworked soil aggregates. The clay coatings we identified in these units present more distinct *laminae* in comparison with the coatings we identified in GL 315 (Fig. 8, detail 1). Based on this difference in internal organization of the fragmented clay coatings we hypothesize that the reworked and redeposited pedofeatures of HS-GU3-4 and HS-GU1 may have formed during two separate and distinct phases of pedogenesis (Kühn et al., 2006).

Soil erosion and deposition of HS-GU3 and 4 was possibly ongoing around 25.000 ^{14}C BP based on dates recovered from the low heat (400 °C) combustion of total organic carbon preserved in the deposits (ID 19, Table 1 B). This may correspond with a phase of deteriorating climate associated with the onset of glacial conditions which likely activated mass-wasting of the regional landscape. It is also possible that the lowering of the valley floor due to the preceding phase of river incision may have promoted hillside instability.

HS-GU3 and 4 were subsequently buried by HS-GU5, which exhibits well-sorted, fine, angular limestone gravel (Fig. 10, detail 1). We interpret this unit as a *Bergkies* deposit (Riek, 1957; Wolff, 1962). HS-GU5 also contains well-rounded aggregates composed of medium and coarse calcite sand coated with alternating laminations of iron stained clay and silt (Fig. 9, detail 2). Similar features have been reported from Pleniglacial deposit in England by Rose et al., (2000), who interpreted them as the result of rolling sand grains mobilized during poorly-drained sheet wash events ("snowball"). Concentric aggregates similar to those we have identified in HS-GU5 have also been identified in deposits influenced by solifluction and gelifluction (Huijzer, 1993; Bertran and Texier, 1999; Van Vliet-Lanoë, 2010).

The radiocarbon age of 25.320 ± 190 ^{14}C BP (ID-19, Table 1 B) from HS-GU4 falls in the range of the Gravettian as published for the Swabian Jura by Conard and Bolus (2008). Therefore, it is possible that the same erosive processes which have been responsible for the deposition of HS-GU3-5 might have also led to the erosion of Gravettian-aged deposits from Hohlenstein-Stadel and other cave sites in The Lone Valley.

Hillside denudation was later followed by accumulation of sheet flow deposition (Blikra and Nemeč, 1998; Pawelec, 2006) represented by HS-GU7 (Fig. 6, HS-GU7, and Fig. 7, detail 7). This unit is the only deposit that we have recovered in front of Hohlenstein that is almost exclusively composed of laminated, reworked loess. The increased presence of loess within this unit may indicate a shift towards colder and drier climate conditions.

4.1.3. Soil formation, river incision, mass-wasting, and floodplain aggradation (Late Glacial to Holocene)

The overlying units HS-GU8, -9 and -10 are composed of

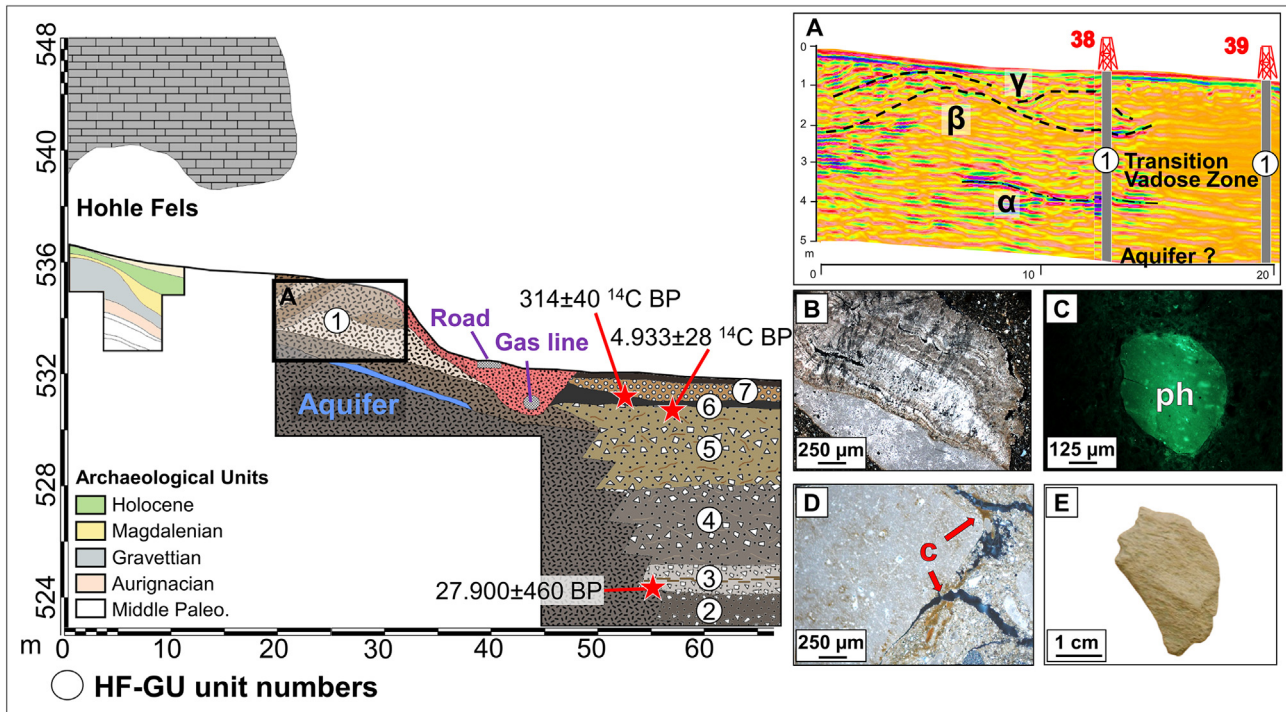


Fig. 15. Section from Hohle Fels cave down into The Ach Valley. This drawing is based on data from the excavations conducted inside the cave (from Maria Malina) and our results from Vorplatz and Ach valley. HF-GUs are numbered on the GPR profile and on the drawing. **A**, GPR profile from the Vorplatz. α , β , γ indicate the main reflected phases which are discussed in the text. **B**, photomicrograph in XPL of a speleothem fragment, from HF-GU2. **C**, photomicrograph in FL of an isolated grain of phosphatized loess, from HF-GU2. **D**, photomicrograph in XPL of reworked limpid clay coatings (**C**). **D**, photo of the bone fragment dated to 27.900 ± 460 ^{14}C BP dating, from HF-GU3.

angular, fresh, coarse to fine, limestone gravel, which we interpret as *Bergkies* (Riek, 1957; Wolff, 1962). These units appear generally very rich in reworked clay coatings, fragmented compound layered coatings, clay aggregates and *in situ* to reworked clay infillings (Fig. 8, detail 4, 5).

In contrast, HS-GU11 is richer in finer grained materials and contains clay pedofeatures that appear to have suffered only minor displacement (Fig. 8, detail 6) or even to have been preserved *in situ*.

The presence of reworked and redeposited clay pedofeatures in the HS-GU8–11 sequence suggests that these sediments may have formed through the periodic alternation of colluviation and weak pedogenesis.

Our GPR data suggests that HS-GU10–11 was partially eroded, likely as a result of river incision. This erosion also explains the absence of HS-GU4–9 in the center of the flood plain (Figs. 6 and 7). We hypothesize that this river incision was later followed by a period of hillside instability. The consequent increase in sediment load from the hillside likely impeded further river incision and promoted flood plain aggradation. In this phase the Lone River deposited the well-rounded to angular, coarse, medium and fine gravel of HS-GU14 (Fig. 6, HS-GU14, and Fig. 7, detail 14). Our GPR data show that this unit exhibits dense, laterally continuous, dipping reflectors comparable with point bar deposits discussed by Aspiron and Aigner (1999) and Bridge (et al., 1995 and 2009, Fig. 11).

This phase of floodplain aggradation was probably triggered by the accumulation at the foothills of non-decalcified, reworked loess and angular, fresh and fine limestone gravel (HS-GU12, Fig. 10, detail 2). Our GPR data from the north hillside show that this unit is composed of imbricated beds that resemble those described for low-viscosity debris flow relict deposits (Blikra and Nemeč, 1998, Fig. 5, Supplementary material).

We hypothesize that HS-GU12 was affected by laterally

extensive erosion probably during the Holocene (Fig. 11, detail B), as suggested by the pottery fragments from the top HS-GU14 in core 27.

4.2. Landscape formation processes in front of Bockstein in The Lone Valley

Similar to the sequence reconstructed for the Hohlenstein area, the sediments we have recovered from the Lone Valley downhill from the Bockstein complex have formed through alternating phases of landscape stability and erosion.

4.2.1. Soil formation (before 32,000 ^{14}C BP)

BS-GU2 contains the earliest evidence for reworked pedofeatures that we have documented in the Bockstein area. This unit contains a high number of reworked manganese nodules, reworked soil aggregates and redeposited fragmented, laminated clay coatings (Fig. 13, detail A). Accumulation of this reworked soil likely took place between 32.390 ± 450 ^{14}C BP and 28.280 ± 270 ^{14}C BP (Table 1 B).

Integrating our data from Hohlenstein and Bockstein we conclude that probably before 32,000 ^{14}C BP at least some areas of the Lone Valley were covered with a soil in which clay illuviation had taken place. This scenario of landscape stability is also supported by the results of the fauna analysis that Krönneck (2012) conducted on the Aurignacian horizon of Bockstein-Törle (BT VII), where she identified species indicative of steppe and forest environments.

4.2.2. Soil erosion and potential minor cave erosion (32,000 ^{14}C BP - 26,000 ^{14}C BP)

We hypothesize that during a subsequent phase of climate deterioration the lack of arboreal vegetation along the slope may

have triggered mass-wasting. This phase of landscape instability corresponds to the accumulation of BS-GU2 which contains fragmented clay coatings (Fig. 12, BS-GU2, and Fig. 13, detail 2).

In the *Brandplatte* area, uphill from the location of our cores, Wetzel reported a deposit which presented lithological characteristics (particularly dark color and high amount of gravel) comparable with our BS-GU2 (Fig. 13). In this sediment Wetzel also discovered mixed Upper and Middle Paleolithic artefacts, which Bosinski interpreted as colluvial material eroded from the cave of Bocksteinloch (Wetzel and Bosinski, 1969, p. 18). The hypothesis that BS-GU2 might correspond to a phase of cave erosion is not fully supported by our data. In this unit we identified only one sand-sized fragment of bone (Fig. 13, detail B) and one coarse gravel-sized fragment of chert, the latter could come from the local bedrock or could represent a fragment of lithic debitage. Here, we did not identify any phosphatized grains of loess. Moving even further downhill—in the Lone floodplain—Schneidermeier (1999) did not report the recovery of any bones or artefacts in his cores. At the same time, our and Schneidermeier's data cannot reject the possibility that a phase of cave erosion actually occurred at Bockstein between 32,000 ¹⁴C BP - 26,000 ¹⁴C BP. This erosional phase might have been less intensive than in later periods (see next section) and thus might be poorly visible in the sediments preserved at the foot of the hill. Further investigation of the sediments accumulated uphill from our core 31 is today impeded, since these deposits have been largely removed in the course of previous investigations (Wetzel and Bosinski, 1969).

4.2.3. Hillside instability, major cave erosion, major loess deposition (26,000 14C BP - 20,000 14C BP)

Fauna assemblages from the Gravettian horizons of Bockstein-Törle (BT VI-IV) are indicative of a landscape dominated by grasslands and wetlands (Krönneck, 2012). We hypothesize that around the time of the LGM, hillside denudation was still active and might have triggered a major phase of cave erosion.

BS-GU3 is composed of laminated, non-phosphatized reworked loess alternating with occasional beds of medium to fine, sub-rounded limestone gravel (Fig. 12, BS-GU3, and Fig. 13, detail 3). Similar sediments have been reported from various regions of Europe and have been interpreted as the result of alternating sheet and snow-flows (Blikra and Nemeč, 1998; Pawelec, 2006). BS-GU4 has the same composition as BS-GU3 but displays increased mean grain size that might be related to a shift towards higher energy mass-wasting (Fig. 12, BS-GU4, and Fig. 13, detail 4). At the contact between these two units we have identified fragments of bones and phosphatized grains of loess (Fig. 13, details C and D). Associated with these components we have also identified snail shells, which contain well preserved aragonite and yielded an age of 25,900 ± 200 ¹⁴C BP (ID 69, Table 1 B). Due to the potential incorporation of fossil carbon in gastropod shells, this ¹⁴C measurement might be overestimated by 1500 (Yates et al., 2002) to 3120 ¹⁴C years (Goodfriend and Stipp, 1983). However, despite these uncertainties, the range of 26,000–23,000 ¹⁴C BP falls in the interval of 20,000–31,000 ¹⁴C BP published by Conard and Bolus (2003) for the Gravettian horizon BT VI from Bockstein-Törle.

As micromorphological studies were not conducted at the Bockstein caves, it is difficult to identify the cave as a potential source of sediment for the slope and valley deposits. However, detailed micromorphological studies at Hohle Fels (Goldberg et al., 2003; Miller, 2015), Geißenklösterle (Miller, 2015) and Hohlenstein-Stadel (Barbieri and Miller, in press) suggest that Pleistocene-aged deposits found in the local caves are largely composed of phosphatized loess and contain numerous sand-sized fragments of bone. Therefore, we conclude that the bone fragments and phosphatized grains of loess redeposited in BS-GU3 and 4 were

likely eroded from Bockstein-Törle or other cavities of the Bockstein complex.

Similarly to HS-GU7, BS-GU3 and 4 are very rich in reworked loess and appear nearly free of fragmented clay coatings. Therefore we suggest, similarly to the sequence from Hohlenstein, that these three units might represent a shift towards a colder, dryer environment associated with the onset of glacial conditions. Alternatively the absence of these pedofeatures in BS-GU3 and 4 might indicate that the soil originally formed on top of the plateau was completely eroded before the deposition of these units.

4.2.4. River erosion (Late Glacial to Holocene)

BS-GU5 (Fig. 12, BS-GU5, and Fig. 13, detail 5) displays similarities with the *Bergkies* deposits exposed by Wetzel slightly uphill from core 31. In those deposits Wetzel recovered non-diagnostic upper Paleolithic stone tools (Wetzel and Bosinski, 1969).

Our GPR data suggest that BS-GU5 exhibits structural analogies with HS-GU12 (Fig. 5 in Supplementary material). Both of these deposits display imbricated bedding comparable to that reported by Blikra and Nemeč (1998) from debris flow deposits in Norway. Our GPR data also indicate that this unit was partially eroded, likely by the Lone River which also subsequently covered this discontinuity with fine, alluvial sediment.

4.3. Landscape formation processes in front of Hohle Fels in the Ach valley

The data collected in the area around Hohle Fels suggests that the Ach Valley also experienced several phases of soil formation, river incision, hillside denudation and loess accumulation.

4.3.1. River incision, soil and cave erosion, major loess deposition (after 28,000 14C BP)

Some hundred meters northwards from our core 37, Groschopf (1973) recovered core 7624/45 (Fig. 5, detail 3), which yielded sediments similar to HF-GU2 to HF-GU7 (Fig. 6 in Supplementary material). For example, our HF-GU6 exhibits color, composition and depth-below-surface that is comparable with a dark peat recovered by Groschopf at 2.8 m underground. Below this, to a depth of -5.2 m, he described a sequence composed of yellow-brown silty-sand, which is similar to what we described for HF-GU5. Additionally, to a depth of -14 m, Groschopf reported gravel that was embedded in gray matrix which is possibly equivalent to HF-GU2-4. In core 7624/45, underneath these deposits (-14 m) Groschopf recovered a thick marl covering Alpine gravel, the latter was probably deposited in the Ach Valley by the palaeo-Danube. Additional coring and geophysical data indicate that this marl deposit is laterally continuous in the Ach and Schmiech valleys and was partly eroded during a phase of valley incision (Brost et al., 1987; German et al., 1995, Fig. 7 in Supplementary material, lower detail). If we accept the correlation of HF-GU2 with the sequence described by Groschopf, we can conclude that HF-GU2 might have been deposited shortly after a phase of river valley incision.

In HF-GU2 we found sand-sized grains of phosphatized loess together with fragments of bone, speleothems and rare reworked clay coatings (Fig. 15, detail B, C and D). Previous micromorphological investigations conducted inside Hohle Fels show that the cave sediments are largely composed of loess that has been either decalcified or phosphatized (Goldberg et al., 2003; Miller, 2015). We conclude that the most likely source for the phosphatized grains of loess, speleothem and bone fragments deposited in HF-GU2 is the nearby cave of Hohle Fels and that unit HF-GU2 formed as a result of mass-wasting that originated from both the external hillside and Hohle Fels cave.

In the lower part of HF-GU3 we recovered a medium gravel-sized fragment of bone dated to ca 28.000 ¹⁴C BP (ID 63, Table 1 B, Fig. 15, detail E). Although the bone still contained collagen enough for the radiocarbon measurement (Table 1 A), the edges of this bone appear subrounded indicating that it has been reworked. This hypothesis is supported also by the dimension of the bone fragment which is within the average size of the limestone gravel in which it was buried. Based on these observation we hypothesize that it has been possibly eroded from the nearby cave deposits. The age of 28.000 ¹⁴C BP falls in the interval of 29.000–26.000 ¹⁴C BP published for the Gravettian occupation of The Ach Valley by Conard and Moreau (2004), Conard and Bolus (2008) and Moreau (2010). Therefore we conclude that this bone fragment might have been eroded from the Gravettian sediments accumulated inside the cave of Hohle Fels. Interestingly, our results support previous geoarchaeological investigations conducted within this cave which hypothesized the partial erosion of Gravettian deposits (Miller, 2015).

In The Ach Valley cave erosion was later followed by the deposition of HF-GU5 (Fig. 14, HF-GU5, and Fig. 15, detail 5) which is composed of graded laminations of well-sorted, non-decalcified, coarse, reworked loess. In this unit fragments of limestone gravel and clay coatings are rare.

4.3.2. Hillside and cave erosion (possibly Late Glacial)

Our GPR data from the *Vorplatz* of Hohle Fels revealed a large erosive disconformity located approximately 1–2 m below the ground surface that separates lower poorly stratified sediments from upper, more densely stratified deposits (Fig. 15, detail A.β). These sediments are composed of loose, angular, fine to coarse limestone gravel alternating with non-decalcified, reworked loess, which we interpret as *Bergkies* (Riek, 1957; Wolff, 1962).

Similar sequences have been documented along the slopes of various regions where periods of intense rock fall have alternated with channel-scouring events, triggered by sudden snow melt or thunderstorms (Van Steijn et al., 1995; Blikra and Nemeč, 1998; Wilkerson and Schmid, 2003; Sass and Krautblatter, 2007; Onaca et al., 2016). The disconformity we have documented at the *Vorplatz* dips also towards the cave entrance where water coming from the cave in the form of sheet flow might have joined sheet/debris flows active along the slope. This disconformity is overlain by beds of gravel that dip towards both the cave entrance and the center of the Ach Valley (Fig. 15, detail A.γ). An illegal excavation conducted along the rock face close to the cave entrance exposed Magdalenian-aged material likely buried within this deposit (Blumentritt personal communication).

4.3.3. River erosion (Mid-Holocene)

HF-GU6 represents the youngest evidence for major landscape change in the Ach Valley (Fig. 14, HF-GU6, and Fig. 15, detail 6). We hypothesize that this unit results from cycles of peat accumulation and erosion similar to those reconstructed by Rittweger (2000) for the “Black Floodplain Soil”, which is commonly reported from river valleys across Germany. ¹⁴C measurements performed on the carbon extracted by low heat combustion (400 °C) of sample ID-58 (Table 1 B) suggest that HF-GU6 began accumulating around 5.000 ¹⁴C BP together with reworked loess and other mineral components. This depositional process lasted probably until a few centuries ago (ID 57, Table 1 B). Today this deposit appears laterally discontinuous in the Ach, Blau and Schmiech valleys (Groschopf, 1973; Gwinner, 1989).

5. Major landscape processes and their impact on cave sequences

5.1. Significance of the fragmented clay coatings

In most of our Geological Units we have identified numerous reworked and fragmented, laminated clay coatings. Such pedofeatures originate from multiple cycles of clay illuviation and are regarded as indicators of long-lasting landscape stability (Kühn et al., 2010). *In situ* clay coatings have been reported from paleosols formed across Europe during colder (Sedov et al., 2013) or warm Interstadials of the Late Glacial (Van Vliet-Lanoë, 1990; Kühn, 2003). Fragmented clay coatings have been documented in various Würm-aged colluvial sediments (Buch and Zöller, 1990; Antoine et al., 2001; Kühn et al., 2006; Sedov et al., 2013). In particular Van Vliet-Lanoë (1990) has discussed the role of gelifluction as potential process responsible for the disruption and deposition of these pedofeatures.

We propose that the reworked and fragmented clay coatings we have observed in our GUs might have been the result of different processes. The clay pedofeatures of HS-GU4 and 5 might have been disrupted and deposited by gelifluction. In support of this hypothesis, we have also observed granostriated b-fabric and well-rounded, concentric aggregates of silt and clay (Fig. 9, detail 1). These features are comparable with the cryogenic microfibrils described by Huijzer (1993) and Van Vliet-Lanoë (2010). In apparent contradiction with this interpretation, HS-GU4 and 5 do not display micromorphological features indicative for ice segregation (e.g. banded microfabric or platy microstructure), which, on the contrary, have been observed in Pleniglacial and LGM cave deposits of both Lone and Ach valleys (Goldberg et al., 2003; Miller, 2015; Barbieri and Miller, in press). This absence is likely due to the higher presence of gravel (for instance in HS-GU5, Van Vliet-Lanoë, 2010) and the more intensive reworking that these open-air sediments might have undergone in comparison with the cave deposits. The fragmented clay coatings we have observed in the remaining GUs of both Ach and Lone valleys are not associated with potential cryogenic microfibrils, banded microfabric nor platy microstructure. Therefore, other mass-wasting processes (such as debris flow) might have been responsible for the deposition of these sediments.

5.2. Phases of soil formation, soil erosion, river valley incision, soil and cave erosion

From the Lone Valley Schneidermeier (1999) recovered “red horizons” which he interpreted as potential paleosols preserved *in situ*. In contrast, our micromorphological results indicate that these deposits are likely formed from redeposited soil material. GL 315 within HS-GU1 displays fragments of dusty clay coatings and thus represents the earliest evidence for soil formation and denudation in our study region (Fig. 8, detail 1 and 2). Our data do not clarify the age of this deposit (Fig. 16). Results from our geophysical measurements show that HS-GU1 might have been eroded in the course of a phase of river valley incision, which lowered the Lone Valley floor of about 3.5 m (Fig. 7 in the text, Fig. 7 in Supplementary material). Interestingly, in the Ach and Schmiech valleys Brost et al. (1987) and German et al. (1995) documented a comparable major valley incision, which lowered the floor of these two valleys of ca. 10 m (incision of marl deposits in Figs. 6 and 7 in Supplementary material). The lack of dating for the deeper deposits preserved in Ach and Lone valleys make the correlation of these disconformities tentative (Fig. 16).

On top of these river incisions, in HS-GU3-4 (Fig. 8, detail 3), BS-GU2 (Fig. 13, detail A) and HF-GU2 (Fig. 15, detail D) we documented fragmented, limpid clay coatings which present more

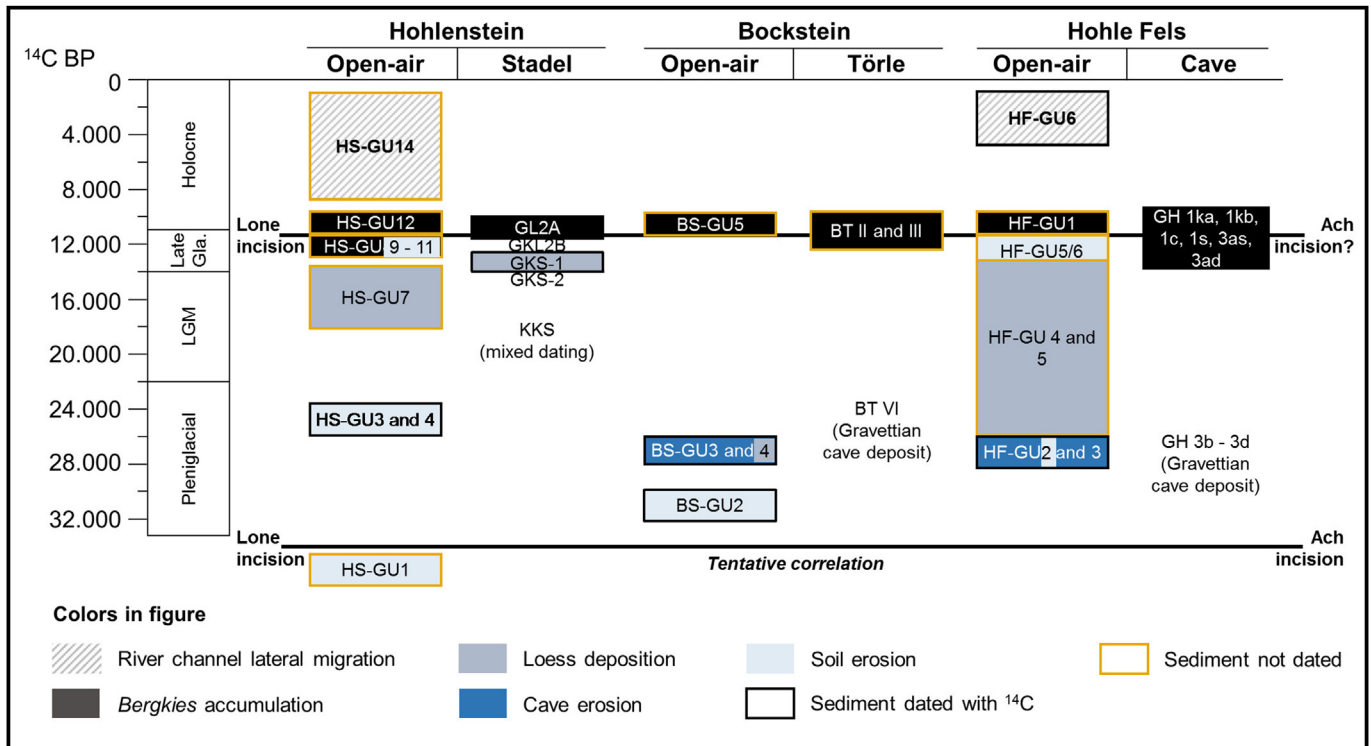


Fig. 16. Timetable. Chronological synthesis of the main geomorphological processes active in the cave sites and in the landscape of Ach and Lone valleys.

distinct laminae in comparison with those deposited in GL 315 (Fig. 8, detail 1). Based on their internal organization, we hypothesize that the pedofeatures redeposited in HS-GU1, on one hand, and HS-GU3-4, BS-GU2 and HF-GU2, on the other hand, might have originated in the course of two distinct phases of soil formation (Kühn et al., 2006). Basing on our ¹⁴C dating, HS-GU3-4, BS-GU2 and HF-GU2 have been deposited in the course of phases of soil erosion, which took place in Ach and Lone valleys between 32.000 and 25.000 ¹⁴C BP (Fig. 16).

In partial overlap with these phases of soil erosion (Fig. 16), Gravettian-aged sediments (BS-GU3-4 and HF-GU2-3) containing grains of phosphatized loess (Fig. 13, detail C and D. Fig. 15, detail C), fragments of speleothem (Fig. 15, detail B), and bone fragments (Fig. 13, detail D. Fig. 15, detail E) were eroded and redeposited in front of the caves of Bockstein and Hohle Fels. Interestingly, our results support the observations of Miller (2015), who hypothesized the presence of erosive contacts within the Gravettian deposit of Hohle Fels. From the area opposite from Hohlenstein we did not recover any material potentially eroded from this cave complex. This is to be expected since the area we have covered with our survey and coring is located on the other side of the Lone River, at a distance of about 150 m from the cave entrances and slightly upstream in comparison with Hohlenstein. Nevertheless, previous archaeological investigations showed that also the Gravettian deposits accumulated within Hohlenstein-Stadel might have suffered major erosion (units KKS and GKS-2 in Figs. 4 and 16. Jahnke, 2013).

In the Ach and Lone valleys, phases of soil formation, river valley incision, soil and cave sediment erosion likely resulted from the adaptation of the vegetation coverage to the climatic changes. We hypothesize that during Würm interstadials the spread of arboreal vegetation might have offered conditions suitable for long-lasting landscape stability and thus soil formation (Jahnke, 2013; Krönneck, 2012; Kitagawa, 2014; Riehl et al., 2015). In the spring and early summer of these periods, the water discharged from the

melting snow drained into the unfrozen ground, possibly causing clay illuviation (Clark, 1988. Fig. 17, detail 1). In the passage from interstadials to stadials the vegetation likely adapted to the climate change with a time lag of some 50–100 years (Knox, 1984; Jump and Peñuelas, 2005). We hypothesize that during these transitional periods, the permafrost table was shallow, melting water was drained in river channels and both hillsides and riversides were stabilized by sparse arboreal coverage (Fig. 17, detail 2). As result, the water discharge would have been higher than the sediment supply (Mol et al., 2000; Van Huissteden and Kasse, 2001). In this hydrological setting, the rivers Lone and Ach might have been able to incise, respectively, HS-GU1 (Fig. 7 in the text and Fig. 7 in Supplementary material) and marl deposits (Figs. 6 and 7 in Supplementary material). After this river incisions, frozen ground and grasslands spread in the Lone and Ach valleys towards the end of the Pleniglacial (Goldberg et al., 2003; Jahnke, 2013; Krönneck, 2012; Kitagawa, 2014; Miller, 2015; Riehl et al., 2015; Barbieri and Miller, in press). We hypothesize that the lack of arboreal vegetation along the hillside together with the lowered base level of the two valleys likely triggered major mass-wasting of soils and cave sediments (Fig. 17, detail 3).

5.3. Shift in sediment source: from reworked soil material to loess

The Gravettian-aged material eroded from the caves of Bockstein was redeposited in a sediment largely composed of reworked loess, with occasional gravel beds and almost free of fragmented clay coatings (BS-GU3 and 4). Similar sediments accumulated also in front of Hohlenstein (HS-GU7) and, after the phase of cave erosion, in front of Hohle Fels (HF-GU5. Fig. 16).

Higher loess sedimentation in the Ach and Lone valleys might be regarded as an indicator of drier and colder climate compatible with the LGM. Additionally, the drop in the amount of reworked clay coatings suggest that the accumulation of these units was not

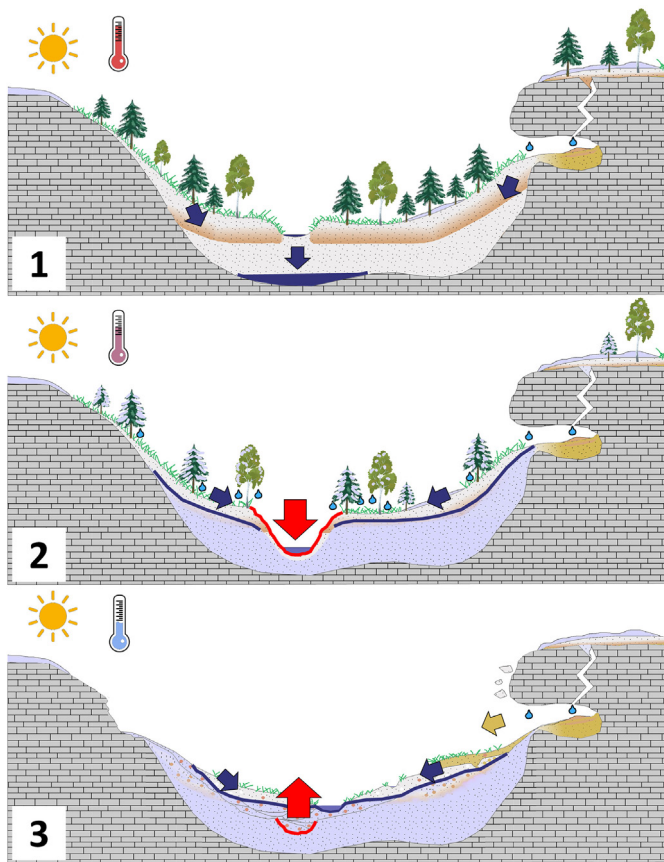


Fig. 17. Landscape formation processes. This figure illustrates the main geomorphological processes which we reconstructed for both Ach and Lone valleys. **1.** phase of climate amelioration with spreading of arboreal vegetation, hillside stability, deeper water drainage (blue arrows) and consequent clay illuviation. **2.** climate deterioration with consequent less dense arboreal coverage, permafrost (blue line), surface water (blue arrows) and valley incision (red arrow). **3.** advanced climate deterioration, spreading of grasslands, hillside and cave erosion (brown arrow), consequent floodplain aggradation (red arrow). (For interpretation of the references to colour in this figure legend, the reader is referred to the web version of this article.)

interrupted by climate ameliorations favorable to soil formation. The near lack of limestone debris in these deposits may indicate a lower frequency of frost cycles, which was possibly caused by temperatures more constantly under 0 °C. The absence of limestone debris might also indicate that bare bedrock was less exposed and/or erosional processes were more surficial, possibly as result of well-developed permafrost.

Landscape instability and extreme climate forced human groups to leave the Swabian Jura probably at the beginning or shortly after the onset of erosion within the cave, around 26.000 ¹⁴C BP (Conard and Bolus, 2003; Moreau, 2009). However, the removal of deposits from this time period make it difficult to identify exactly when the region may have become depopulated. Loess deposition and thus harsh climatic conditions likely lasted until 14.000 ¹⁴C BP, when loess (GKS-1) sterile and free of phosphatic grains accumulated at the Vorplatz of Hohlenstein-Stadel (Jahnke, 2013; Barbieri and Miller, in press). Starting around 13.000 ¹⁴C BP, Magdalenian groups colonized the region during a cool interstadial towards the beginning of the Late Glacial period (Jahnke, 2013; Teller, 2015).

5.4. River incision, minor cave erosion, Bergkies deposition

After the LGM, in both the Ach and Lone valleys, periodic

alternation of stadials and interstadials led to the accumulation of sediments rich in gravel and fragmented clay coatings (HS-GU9-11, BS-GU5, probably HF-GU1. Fig. 16). Previous investigations conducted at the Vorplatz of Hohlenstein-Stadel showed that the Magdalenian deposit GL2B was partly eroded and covered with sediment containing microfauna compatible with a Stadial period (GL2A, Jahnke, 2013). We hypothesize that during the transition between these two climatic phases the Lone River eroded HS-GU4 to HS-GU11 from the center of the valley (Fig. 16). It is possible that this phase of downcutting corresponds to a similarly-aged event reported from The Danube Valley in the Regensburg area, dated to 13.000–9.000 ¹⁴C BP (Heine, 1999; Münzberger, 2005; Schellmann, 2010). Incision of The Lone Valley was followed by the accumulation of Bergkies at the Vorplatz of Hohlenstein-Stadel (GL2A) and probably also along the hillside opposite from the cave (HS-GU12, Fig. 7, detail 12. Fig. 10, detail 2. Fig. 16).

Our data do not support or refute the occurrence of a contemporaneous river incision in the Ach Valley. Nevertheless, at the entrance of Hohle Fels we detected a shallow disconformity filled with Bergkies (Fig. 15, detail A. Fig. 16). This deposit appears to contain rare Magdalenian artifacts (Blumentritt personal communication). Further research is needed to verify the timing of this sequence.

The association of Magdalenian materials and Bergkies has been reported from various sites, such as Sesselfelsgrötte (Freund, 1998), Felsställe (Kind, 1987), Burkhardtshöhle (Riek, 1935), Spitalhöhle (Riek, 1957), Vogelherd (Riek, 1934), Bockstein (Wetzel and Bosinski, 1969), Brillenhöhle (Riek, 1973) and Sirgenstein (Schmidt, 1912). However assuming that the Magdalenian occupation of the Jura took place while Bergkies was deposited in the valleys is questionable. Given that the Magdalenian colonization of the study region took place during an Interstadial (Jahnke, 2013), the presence of sparse arboreal coverage along the hillside should have prevented major denudation processes. In agreement with the data published for Hohlenstein-Stadel (Jahnke, 2013), a major part of the Bergkies reported from Sesselfelsgrötte was deposited probably after the Magdalenian, during a Stadial period (layer B3, Freund, 1998). Inside Hohle Fels Bergkies forms part of the Magdalenian sequence (layer GH 3ad) but appears more abundant in later, possibly Holocene-aged deposits (1ka, 1kb, 1c, 1s, 3as, Fig. 16. Field descriptions from Maria Malina).

We conclude that the exact timing of Bergkies deposition in caves of the Swabian Jura is not clear and further research is needed to address this point. As a working hypothesis, we propose that this sediment type was produced and deposited during Stadial periods of the Late Glacial when the landscape was shaped by major denudation processes. Increased sedimentation rates of Bergkies might indicate more frequent frost cycles and/or more extensive bedrock denudation during the Late Glacial. In the valley floor, accumulation of Bergkies and coarser gravel prevented any further river incision, promoting floodplain aggradation (HS-GU14). Production of frost debris was likely more intensive in the areas surrounding the different Vorplätze, where bedrock was possibly more exposed. Here deposition of Bergkies overprinted cave erosion and filled the cave entrances.

6. Conclusions

Our research demonstrates that cave sequences can be successfully linked with open air sediment archives when the study focuses at both micro- and macroscopic scales on depositional process, sediment source and diagenesis. This success was only achieved by integrating our data with the results from previous archaeological, faunal, botanical, geoarchaeological and micro-morphological investigations carried out in this region. Our results

show that alternating phases of soil formation, hillside denudation, river valley incision and floodplain aggradation have been the major processes active in Lone and Ach valleys throughout the Pleistocene and Holocene (Fig. 16). These processes impacted the prehistoric archaeological record contained within the caves, in particular:

1. River valley incision and subsequent, intensive mass-wasting of the hillsides promoted the erosion of Gravettian-aged deposits from the caves of Bockstein, Hohle Fels and possibly Hohlenstein-Stadel.
2. Increased deposition rates of loess nearly free from gravel and reworked pedofeatures marks in both the Ach and Lone valleys a shift towards colder and drier conditions corresponding with the LGM. Deteriorating climate likely forced Gravettian groups to abandon the Swabian Jura.
3. Magdalenian recolonization of the region took place in a phase of climate amelioration alternating with phases of major hillside instability, minor cave erosion, bedrock denudation and consequent *Bergkies* production.
4. During or after the Magdalenian, *Bergkies* filled the cave entrances marking the cessation of cave erosion.

Acknowledgments

We would like to express our gratitude to the Baden-Württemberg Ministry of Culture and Science that has funded this project. Our field and lab work would have not been possible without the support of Haydar B. Martínez, Felix Bachover, Geraldine Quénéhervé, Viola Schmid, Peter Kloos, Flora C. Schilt, Clemens Schmid, Elmar Schmaltz, Matthias Czechowski and Lucia Leierer. The thin sections published in this paper have been produced by Panos Kritikakis at the Georadar Laboratory of the University of Tübingen. We are thankful to Hartmut Schulz for having hosted us in the Sand Laboratory of the Department of Geosciences at The University of Tübingen. Thanks to Peter Leach, Jen Ort, Jens Hornung and the Georadarforum for having supported our GPR surveys, to Maria Malina for the access to her field descriptions from Hohle Fels, and finally to Marcus Lee and the staff of the University of Arizona AMS Laboratory for their help with the ^{14}C dating. We also would like to acknowledge Peter Kühn, Wolfgang Ufrecht and Frank Schäbitz for their suggestions and remarks. Finally thanks to Diego E. Angelucci and one anonymous reviewer.

Appendix A. Supplementary data

Supplementary data related to this article can be found at <http://dx.doi.org/10.1016/j.quaint.2017.08.002>.

References

- Annan, A.P., 2009. Electromagnetic principles of ground penetrating radar. In: Jol, H.M. (Ed.), *Ground Penetrating Radar: Theory and Applications*. Elsevier, pp. 3–40.
- Antoine, P., Rousseau, D.-D., Zöller, L., Lang, A., Munaut, A.-V., Hatté, C., Fontugne, M., 2001. High-resolution record of the last interglacial-glacial cycle in the Nussloch loess-palaeosol sequences, upper Rhine area, Germany. *Quat. Int.* 76/77, 211–229.
- Aspiron, U., Aigner, T., 1999. Towards realistic aquifer models: three-dimensional georadar surveys of Quaternary gravel deltas (Singen Basin, SW Germany). *Sediment. Geol.* 129, 281–297.
- Barbieri, A., Miller, C., 2017. Rekonstruktion der Fundplatzgenese der Hohlenstein-Stadel Höhle. In: Kind, C.J. (Ed.), *Die Ausgrabungen 2008–2013 in der Stadel-Höhle im Hohlenstein (Lonetal)*. Gemeinde Asselfingen, Alb-Donau-Kreis in press.
- Beaumont, P.B., Vogel, J.C., 2006. On a timescale for the past million years of human history in central South Africa. *South Afr. J. Sci.* 102, 217–228.
- Beck, D., 1999. Das Mittelpaläolithikum des Hohlenstein, Stadel und Bärenhöhle, im Lonetal. R. Habelt, Bonn.
- Bertran, P., Texier, J.-P., 1999. Facies and microfacies of slope deposits. *Catena* 35, 99–121.
- Bertran, P., Coutard, J.-P., Francou, B., Ozouf, J.-C., Texier, J.-P., 1992. Données nouvelles sur l'origine du litage des grèzes: implications paléoclimatiques. *Géogr. physique Quaternaire* 46 (1), 97–112.
- Bertran, P., Coutard, J.-P., Francou, B., Ozouf, J.-C., Texier, J.-P., 1994. New data on Grèzes bedding and their paleoclimatic implications. In: Evans, D.J.A. (Ed.), *Cold Climate Landforms*. John Wiley & Sons, Chichester, pp. 437–454.
- Beutelspacher, T., Ebinger-Rist, N., Kind, C.-J., 2011. Neue Funde aus der Stadelhöhle im Hohlenstein. *Archäologische Ausgrabungen in Baden-Württemberg 2010*. Konrad Theiss Verlag, Stuttgart, pp. 65–70.
- Blikra, L.H., Nemeč, W., 1998. Postglacial colluvium in western Norway: depositional processes, facies and palaeoclimatic record. *Sedimentology* 45, 909–959.
- Bobak, D., Płonka, T., Pottowicz-Bobak, M., Wiśniewski, A., 2013. New chronological data for Weichselian sites from Poland and their implications for Palaeolithic. *Quat. Int.* 296, 23–36.
- Bolus, M., Conard, N.J., 2012. 100 Jahre Robert Rudolf Schmidts "Die diluviale Vorzeit Deutschlands." *Mittl. Ges. für Urgesch.* 21, 63–89.
- Bolus, M., Conard, N.J., Kandel, A.W., 1999. Grabungen vor dem Hohlenstein im Lonetal, Gemeinde Bissingen und Asselfingen, Alb-Donau-Kreis. *Archäologische Ausgrabungen Baden-Württemberg 1998*, 40–47.
- Borges de Magalhães, J.C., 2000. Die Silexartefakte der Fundschichten IV–VII aus dem Bockstein-Törl im Lonetal, Ostalbkreis. Master Thesis. University of Tübingen.
- Braillard, L., Guelat, M., Rentzel, P., 2004. Effects of bears on rockshelter sediments at Tanay Sur-les-Creux, southwestern Switzerland. *Geoarchaeology* 19 (4), 343–367.
- Bridge, J., 2009. Advances in fluvial sedimentology using GPR. In: Jol, H.M. (Ed.), *Ground Penetrating Radar: Theory and Applications*. Elsevier, printed in Slovenia, pp. 323–359.
- Bridge, J., Alexander, J., Collier, R.E.L., Gawthorpes, R.L., Jarvis, J., 1995. Ground penetrating radar and coring used to study the large-scale structure of point-bar deposits in three dimensions. *Sedimentology* 42, 839–852.
- Brost, E., Homilius, J., Koschyk, K., Villingner, E., 1987. Der Schmiecher See bei Schelklingen Geophysikalische und geologische Untersuchungen zur Erkundung seiner Entstehung. *Geol. Jahrb. (Reihe C)* 49, 38–60.
- Buch, M.W., Zöller, L., 1990. Gliederung und Thermolumineszenz-Chronologie der Würmlösse im Raum Regensburg. *E&G Quat. Sci. J.* 40, 63–84.
- Burr, G.S., Edwards, R.L., Donahue, D.J., Druffel, E.R.M., Taylor, F.W., 1992. Mass spectrometric ^{14}C and U–Th measurements in coral. *Radiocarbon* 34 (3), 611–618.
- Campen, I., 1990. Die Sedimente der Höhlen und Abris der Mittleren Schwäbischen Alb und ihre klimatische Ausdeutung. Universitätsbibliothek Publikation, Tübingen.
- Castel, J.-C., Liolios, D., Chadelle, J.-P., Geneste, J.-M., 1998. De l'alimentaire et du technique: la consommation du renne dans le Solutréen de la grotte de Combe Saunière. In: Antipolis, Sophia (Ed.), *Économie Préhistorique: les comportements de subsistance au Paléolithique – XVIII Rencontres Internationales d'Archéologie et d'Histoire d'Antibes*. APDCA, pp. 433–450.
- Çep, B., Waiblinger, J., 2001. The Use of Cave and Open-air Sites in Southern Germany. Kerns Verlag Tübingen, Tübingen.
- Chazan, M., Ron, H., Matmon, A., Porat, N., Goldberg, P., Yates, R., Avery, M., Sumner, A., Horwitz, L., 2008. Radiometric dating of the earlier stone age sequence on excavation I at Wonderwerk cave, South Africa: preliminary results. *J. Hum. Evol.* 55, 1–11.
- Clark, M.J., 1988. *Advances in Periglacial Geomorphology*. John Wiley & Sons Ltd, Great Britain.
- Conard, N.J., 2001. Advances and problems in the study of paleolithic settlement systems. In: Conard, N.J. (Ed.), *Settlement Dynamics of the Middle Paleolithic and Middle Stone Age*. Tübingen Publications in Prehistory 1. Kerns Verlag Tübingen, pp. VII–XX.
- Conard, N.J., Bolus, M., 2003. Radiocarbon dating the appearance of modern humans and the timing of cultural innovations in Europe: new results and new challenges. *J. Hum. Evol.* 44, 331–371.
- Conard, N.J., Bolus, M., 2008. Radiocarbon dating the late middle paleolithic and the Aurignacian of the Swabian Jura. *J. Hum. Evol.* 55, 886–897.
- Conard, N.J., Moreau, L., 2004. Current research on the Gravettian of the Swabian Jura. *Mittl. Ges. für Urgesch.* 13, 29–59.
- Conard, N.J., Bolus, M., Dutkiewicz, E., Wolf, S., 2015. *Eiszeitarchäologie auf der Schwäbischen Alb*. Kerns Verlag Tübingen.
- Courty, M.A., Vallverdú, J., 2001. The microstratigraphic record of abrupt climate changes in cave sediments of the Western Mediterranean. *Geoarchaeology* 16, 467–499.
- Davids, J.L., Annan, A.P., 1989. Ground-penetrating radar for high-resolution mapping of soil and rock stratigraphy. *Geophys. Prospect.* 37, 531–551.
- Dongus, H., 1974. Die Oberflächenformen der Schwäbischen Alb. *Abhandlungen zur Karst- und Höhlenkunde*. Reihe A, Heft 11. Fr. Mangoldsche Buchhandlung, Blaubeuren. Munich.
- Faith, T., 2007. Changes in reindeer body part representation at Grotte XVI, Dordogne, France. *J. Archaeol. Sci.* 34, 2003–2011.
- Floss, H., Hoyer, C., Dutkiewicz, E., Frick, J., Poenicke, H.-W., 2012. Eine neu entdeckte paläolithische Freilandfundstelle auf der Schwäbischen Alb – Sondagerungen in Börslingen. *Archäologische Ausgrabungen Baden-Württemberg 2011*, 71–73.
- Fraas, O., 1862. *Der Hohlenstein und der Höhlenbär*. Jahreshefte des Vereins für

- vaterländische Naturkunde Württemberg 18, 156–188.
- Freund, G., 1998. Sesselfelsgrötte I: Grabungsverlauf und Stratigraphie. Quartär-Bibliothek, Saarbrücker Druckerei und Verlag, Saarbrücken.
- Geiling, J.M., Bolus, M., Conard, N.J., 2015. The archaeological significance of the Reindeer antlers from the Hohlenstein-complex in the Lone valley of south-western Germany. *Mittl. Ges. für Urgesch.* 24, 97–119.
- German, R., Grüger, E., Schreiner, A., Strayle, G., Villinger, E., 1995. Geologie: Die Entstehung des Schmiechener Sees aufgrund der Bohrung "Schmiechener See 1". In: Hölzinger, J., Schmid, G. (Eds.), *Der Schmiechener See – Naturkunde eines Naturschutzgebietes auf der Schwäbischen Alb*, pp. 31–98. Beihefte zu den Veröffentlichungen für Naturschutz und Landschaftspflege in Baden-Württemberg 78.
- Geyer, F.O., Gewinner, M.P., 1991. Geologie von Baden-Württemberg. E. Schweizerbart'sche Verlagsbuchhandlung (Nägele u. Obermiller), Stuttgart.
- Goldberg, P., 1979. Micromorphology of Pech de l'Azé II sediments. *J. Archaeol. Sci.* 6, 17–47.
- Goldberg, P., Schiegl, S., Meline, K., Dayton, C., Conard, N.J., 2003. Micromorphology and site formation at Hohle Fels cave, Swabian Jura, Germany. *E&G Quat. Sci. J.* 53, 1–25.
- Goldberg, P., Berna, F., Chazan, M., 2015. Deposition and diagenesis in the earlier stone age of Wonderwerk cave, excavation 1, South Africa. *Afr. Archaeol. Rev.* 32, 613–643.
- Goodfriend, G.A., Stipp, J.J., 1983. Limestone and the problem of radiocarbon dating of land-snail shell carbonate. *Geology* 11, 575–577.
- Groschopf, P., 1973. Geologischer Bau. Der Stadt- und der Landkreis Ulm. Amtlicher Kreisbeschreibung, Süddeutsche Verlagsgesellschaft, pp. 5–38.
- Gwinner, M.P., 1989. Erläuterungen zu Blatt 7524 Blaubeuren. Geologische Karte von Baden-Württemberg. Landesvermessungsamt Baden-Württemberg, Stuttgart.
- Hahn, J., 1978. Die altsteinzeitliche Schichtenfolge des „Geißenklösterle“ bei Blaubeuren nach der Grabung 1977. In: *Archäologische Ausgrabungen Baden-Württemberg 1977*, pp. 7–10.
- Hatté, C., Pessenda, L.C., Lang, A., Paterne, M., 2001. Development of accurate and reliable ¹⁴C chronologies for loess deposits: application to the loess sequence of Nussloch (Rhine valley, Germany). *Radiocarbon* 43 (2B), 611–618.
- Heine, K., 1999. Fluvial response of the Danube river to climate change in Bavaria during the Weichselian and the Holocene. *Bol. Goiano Geogr.* 19 (1), 82–93.
- Hoffmann, S., Beilecke, T., Werban, U., Leven, C., Engeser, B., Polom, U., 2008. Joint application of shear wave seismic and direct push methods in the site investigation of an urban aquifer. *Grundwasser* 13 (2), 78–90.
- Huijzer, A.S., 1993. Cryogenic Microfabrics and Macrostructures: Interrelations, Processes and Palaeoenvironmental Significance. PhD-Thesis. Vrije Universiteit Amsterdam.
- Jahnke, T., 2013. Vor der Höhle. Zur Fundplatzgenese am Vorplatz des Hohlenstein-Stadle (lonetal). Unpublished Master Thesis. University of Tübingen.
- Jochim, M., Herhahn, C., Starr, H., 1999. The Magdalenian colonization of southern Germany. *Am. Anthropol.* 101 (1), 129–142.
- Jull, A.J.T., Burr, G.S., Hodgins, G.W.L., 2013. Radiocarbon dating, reservoir effects, and calibration. *Quat. Int.* 299, 64–71.
- Jump, A.S., Peñuelas, J., 2005. Running to stand still: adaptation and the response of plants to rapid climate change. *Ecol. Lett.* 8, 1010–1020.
- Karkanas, P., 2010. Geology, stratigraphy, and site formation processes of the upper paleolithic and later sequence in Klissoura cave 1. *Eurasian Prehistory* 7 (2), 15–36.
- Karkanas, P., Rigaud, J.-P., Simek, J.F., Albert, R.M., Weiner, S., 2002. Ash bones and Guano: a study of the minerals and phytoliths in the sediments of Grotte XVI, Dordogne, France. *J. Archaeol. Sci.* 29, 721–732.
- Karkanas, P., White, D., Lane, C.S., Stringer, C., Davies, W., Cullen, V.L., Smith, V.C., Ntinou, M., Tsartsidou, G., Kyriakou-Apitolika, N., 2015. Tephra correlations and climatic events between the MIS6/5 transition and the beginning of MIS3 in Theopetra Cave. *Quat. Sci. Rev.* 118, 170–181.
- Kind, C.J., 1987. Das Felsställe. Landesamt Baden-Württemberg. Konrad Theiss Verlag Stuttgart.
- Kind, C.J., 2003. Die absolute Datierung des Magdalenines und des Mesolithikums in Süddeutschland. *Veröffentlichungen Des. Landesamtes für Archäologie* 57, 303–319.
- Kind, C.-J., Beutelspacher, T., 2010. Ausgrabungen 2009 im Stadel am Hohlenstein im Lonetal. *Archäologische Ausgrabungen in Baden-Württemberg 2009*. Konrad Theiss, Stuttgart, pp. 62–69.
- Kind, C.J., Ebinger-Rist, N., Wolf, S., Beutelspacher, T., Wehrberger, K., 2014. The smile of the Lion man. Recent excavations in Stadel cave (Baden-Württemberg, south-western Germany) and the restoration of the famous upper paleolithic figurine. *Quartär* 61, 129–145.
- Kitagawa, K., 2014. Exploring Hominins and Animals in the Swabian Jura: Study of Paleolithic Fauna from Hohlenstein-stadel. *Universitätsbibliothek Publikation*, Tübingen.
- Knox, J.C., 1984. Responses of river systems to Holocene climates. In: Wright, H.E. (Ed.), *Late Quaternary Environments of the United States*. Longman, London, pp. 26–41.
- Kösel, M., 2016. Paläoböden in quartärgeologischen Sequenzen und als Bestandteile des Solums rezenter Oberflächenböden – Beispiele aus dem Grenzbereich von Schichtstufenlandschaft und Alpenvorland (Südrand Schwäbische Alb, Donautal, nördliche Iller-Riß-Platte). Technical Report. Landesamt für Geologie, Rohstoffe und Bergbau, Freiburg.
- Krönneck, P., 2012. Die pleistozäne Makrofauna des Bocksteins (Lonetal – Schwäbische Alb) Ein neuer Ansatz zur Rekonstruktion der Paläoumwelt. *Universitätsbibliothek Publikation*, Tübingen.
- Kühn, P., 2003. Micromorphology and late glacial/Holocene genesis of Luvisols in Mecklenburg–Vorpommern (NE-Germany). *Catena* 54, 537–555.
- Kühn, P., Terhorst, B., Ottner, F., 2006. Micromorphology of middle Pleistocene paleosols in northern Italy. *Quat. Int.* 156–157, 156–166.
- Kühn, P., Aguilar, J., Miedema, R., 2010. Textural pedofeatures and related horizons. In: Stoops, G., Marcellino, V., Mees, F. (Eds.), *Interpretation of Micromorphological Features of Soils and Regoliths*. Elsevier, The Netherlands, pp. 149–194.
- Leesch, D., Müller, W., Nielsen, E., Bullinger, J., 2012. The Magdalenian in Switzerland: Re-colonization of a newly accessible landscape. *Quat. Int.* 272–273, 191–208.
- Leven, C., Weiss, H., Wienken, T., Dietrich, P., 2011. Direct Push technologies-an efficient investigation method for subsurface characterization. *Grundwasser* 16 (4), 221–234.
- Lindbo, D.L., Stolt, M.H., Vepraskas, M.J., 2010. Redoximorphic features. In: Stoops, G., Marcellino, V., Mees, F. (Eds.), *Interpretation of Micromorphological Features of Soils and Regoliths*. Elsevier, The Netherlands, pp. 129–147.
- Lin-Vien, D., Colthup, N.B., Fateley, W.G., Grasselli, J.G., 1991. *The Handbook of Infrared and Raman Characteristic Frequencies of Organic Molecules*. Academic Press, London.
- Litt, T., Brauer, A., Goslar, T., Merkt, J., Baigal, K., Müller, H., Raiska-Jasiewiczowa, M., Stebich, M., Negendank, J.F.W., 2001. Correlation and synchronization of Lateglacial continental sequences in northern central Europe based on annually laminated lacustrine sediments. *Quat. Sci. Rev.* 20, 1233–1249.
- Lu, Q., Sato, M., 2007. Estimation of hydraulic property of an unconfined aquifer by GPR. *Sens. Imaging Int. J.* 8 (2), 83–99.
- Malan, B.D., Cooke, H.B.S., 1941. A preliminary account of the Wonderwerk cave, Kuruman District, South Africa. *South Afr. J. Sci.* 37, 300–312.
- McGeehin, J., Burr, G.S., Jull, A.J.T., Reines, D., Gosse, J., Davis, P.T., Muhs, D., Southon, J.R., 2001. Stepped-combustion ¹⁴C dating of sediment: a comparison with established techniques. *Radiocarbon* 43 (2A), 255–261.
- Mentzer, S.M., 2011. Macro- and Micro-scale Geoarchaeology of Ucagizli Caves I and II. The University of Arizona, Hatay, Turkey.
- Miller, C.E., 2015. A Tale of Two Swabian Caves – Geoarchaeological Investigations at Hohle Fels and Geißenklösterle. *Kerns Verlag Tübingen*.
- Mol, J., Vandenberghe, J., Kasse, C., 2000. River response to variations of periglacial climate in mid-latitude Europe. *Geomorphology* 33, 131–148.
- Moreau, L., 2009. Geißenklösterle. *Das Gravettien der Schwäbischen Alb im europäischen Kontext*. *Kerns Verlag Tübingen*.
- Moreau, L., 2010. Geißenklösterle. *The Swabian Gravettian in its European context*. *Quartär* 57, 79–93.
- Münzberger, P., 2005. Jungquartäre Talgeschichte der Donau und ihrer Nebenflüsse im Raum Straubing – Deggendorf in Abhängigkeit von natürlichen und anthropogenen Einflüssen. In: *Regensburger Beiträge zur Bodenkunde, Landschaftsökologie und Quartärforschung*, vol. 8. Regensburg.
- Niven, L., 2007. From carcass to cave: large mammal exploitation during the Aurignacian at Vogelherd, Germany. *J. Hum. Evol.* 53, 362–382.
- Onaca, A., Ardelean, A.C., Urdea, P., Ardelean, F., Sărășan, A., 2016. Genetic typologies of talus deposits derived from GPR measurements in the Alpine Environment of the Făgăraș Mountains. *Carpathian J. Earth Environ. Sci.* 11 (2), 609–616.
- Ozouf, J.-C., Coutard, J.-P., Lautridou, J.-P., 1995. Grèzes, Grèzes Littées: Historique des Définitions. *Permafrost, Periglac. Process.* 6, 85–87.
- Pawelec, H., 2006. Origin and palaeoclimatic significance of the Pleistocene slope covers in the Cracow Upland, southern Poland. *Geomorphology* 74, 50–69.
- Pessenda, L.C.R., Gouveia, S.E.M., Aravena, R., 2001. Radiocarbon dating of total soil organic material and humin fraction and its comparison with ¹⁴C ages of fossil charcoal. *Radiocarbon* 43 (2B), 595–601.
- Pirson, S., Flas, D., Abrams, G., Bonjean, D., Court-Picon, M., Di Modica, K., Draily, C., Damblon, F., Haesaerts, P., Miller, R., Rougier, H., Toussaint, M., Semal, P., 2012. Chronostratigraphic context of the middle to upper paleolithic transition: recent data from Belgium. *Quat. Int.* 259, 78–94.
- Riehl, S., Marinova, E., Deckers, K., Malina, M., Conard, N.J., 2015. Plant use and local vegetation patterns during the second half of the Late Pleistocene in south-western Germany. *Archaeol. Anthropol. Sci.* 7 (2), 151–167.
- Riek, G., 1934. Die Eiszeitjägerstation am Vogelherd im Lonetal I: Die Kulturen. *Akademische Verlagsbuchhandlung Franz F. Heine, Tübingen*.
- Riek, G., 1935. *Kulturbilder aus der Altsteinzeit Württembergs*. Franz. F. Heine, Verlagsbuchhandlung, Tübingen.
- Riek, G., 1957. Drei jungpaläolithische Stationen am Bruckersberg in Giengen an der Brenz. *Veröffentlichungen des Staatlichen Amtes für Denkmalpflege Stuttgart*, Verlag Silberburg – Kommissionsverlag, Stuttgart.
- Riek, G., 1973. *Das Paläolithikum der Brillenhöhle bei Blaubeuren (Schwäbische Alb) I*. *Landesdenkmalamt Baden-Württemberg, Verlag Müller & Gräff – Kommissionsverlag Stuttgart*.
- Rittweger, H., 2000. The "black floodplain soil" in the Amöneburger Becken, Germany: a lower Holocene marker horizon and indicator of an upper Atlantic to subboreal dry period in central Europe? *Catena* 41 (1–3), 143–164.
- Rose, J., Lee, J.A., Kemp, R.A., Harding, P.A., 2000. Paleoclimate, sedimentation and soil development during the last glacial stage (Devensian), Heathrow Airport, London, UK. *Quat. Sci. Rev.* 19, 827–847.
- Saladié, P., Huguet, R., Díez, C., Rodríguez-Hidalgo, A., Cárceres, I., Vallverdú, J., Rosell, J., Bermúdez de Castro, J.M., Carbonell, E., 2011. Carcass transport decisions in Homo antecessor subsistence strategies. *J. Hum. Evol.* 61, 425–446.

- Sanz, M., Daura, J., Égüez, N., Brugal, J.-P., 2016. Not only hyenids: a multi-scale analysis of Upper Pleistocene carnivore coprolites in Cova del Coll Verdaguer (NE Iberian Peninsula). *Paleogeogr. Paleoclimatol., Paleoecol.* 443, 249–262.
- Sass, O., Krautblatter, M., 2007. Debris-flow-dominated and rockfall-dominated scree slopes: genetic models and process rates derived from GPR measurements. *Geomorphology* 86 (1), 176–192.
- Sauer, D., Kadereit, A., Kühn, P., Miller, E.C., Shinonaga, T., Kreutzer, S., Hermann, L., Fleck, W., Starkovich, B.M., Stahr, K., 2016. The loess-paleosol sequence of Datthausen, SW Germany: characteristics, chronology, and implications for the use of the Lohne Soil as a marker soil. *Catena* 146, 10–29.
- Schall, W., 2002. Erläuterungen Zum Blatt 7425 Lonsee. Geologische Karte von Baden-Württemberg. Landesvermessungsamt Baden-Württemberg, Stuttgart.
- Schellmann, G., 2010. Neue Befunde zur Verbreitung, geologischen Lagerung und Altersstellung der würmzeitlichen (NT 1 bis NT3) und holozänen (H1 bis H7) Terrassen im Donautal zwischen Regensburg und Bogen. *Bamb. Geogr. Schriften* 24, 1–77.
- Schiegl, S., Goldberg, P., Pfretzschner, H.-U., Conard, N., 2003. Paleolithic burnt bone horizons from the Swabian Jura: distinguishing between in situ fireplaces and dumping areas. *Geoarchaeology* 18, 541–565.
- Schmidt, R.R., 1912. Die Diluviale Vorzeit Deutschlands. E. Schweizerbartsche Verlagsbuchhandlung Nägele und Dr. Spoesser, Stuttgart.
- Schneidermeier, T., 1999. Paläolithische Fundschichten in quartären Locksedimenten (Südwestdeutschland): Prospektionsmethoden, Stratigraphie und Paläoökologie. *Tübinger Geowissenschaftliche Arbeiten (Reihe A, Band 57)*. Attempto Service GmbH, Tübingen.
- Schulmeister, M.K., Butler, J.J., Healey, J.M., Zheng, L., Wysocki, D.A., McCall, G.W., 2003. Direct-push electrical conductivity logging for high-resolution hydrostratigraphic characterization. *Ground Water Monit. Remediat.* 23 (3), 52–62.
- Sedov, S., Sycheva, S., Targulian, V., Pi, T., Díaz, J., 2013. Last Interglacial paleosols with Argic horizons in Upper Austria and Central Russia – pedogenetic and paleoenvironmental inferences from comparison with the Holocene analogues. *E&G Quat. Sci. J.* 62 (1), 44–58.
- Shahack-Gross, R., Berna, F., Karkanas, P., Weiner, S., 2004. Bat guano and preservation of archaeological remains in cave sites. *J. Archaeol. Sci.* 31, 1259–1272.
- Sherwood, S., Driskell, B.N., Randall, A.R., Meeks, S.C., 2004. Chronology and stratigraphy at dust cave, Alabama. *Am. Antiq.* 69, 533–554.
- Starkovich, B.M., 2014. Optimal foraging, dietary change, and site use during the Paleolithic at Klissoura Cave 1 (southern Greece). *J. Archaeol. Sci.* 52, 39–55.
- Stoops, G., 2003. Guidelines for Analysis and Description of Soil and Regolith Thin Sections. Soil Science Society of America, Inc, Madison, Wisconsin, USA.
- Strasser, M., Strasser, A., Pelz, K., Seyfried, H., 2009. A mid Miocene to early Pleistocene multi-level cave as a gauge for tectonic uplift of the Swabian Alb (Southwest Germany). *Geomorphology* 106, 130–141.
- Taller, A., 2015. Das Magdalenien des Hohle Fels: Chronologische Stellung, Lithische Technologie und Funktion der Rückenmesser. Kerns Verlag Tübingen.
- Terberger, T., 2003. Vom Gravettien zum Magdalénien in Mitteleuropa – Aspekte der menschlichen Besiedlungs- geschichte in der Zeit um das zweite Kältemaximum der letzten Eiszeit. *Archäologisches Nachrichtenblatt* 8, 55–62.
- Terhorst, B., Kühn, P., Damm, B., Hambach, U., Meyer-Heintze, S., Sedov, S., 2014. Paleoenvironmental fluctuations as recorded in the loess-paleosol sequence of the Upper Paleolithic site Krems-Wachtberg. *Quat. Int.* 351, 67–82.
- Ufrecht, W., 2008. Evaluating landscape development and karstification of the Central Schwäbische Alb (Southeast Germany) by fossil record of karst fillings. *Z. für Geomorphol.* 52 (4), 417–436.
- Vanderberghe, J., 2015. River terraces as response to climate forcing: formatting processes, sedimentary characteristics and sites for human occupation. *Quat. Int.* 370 (3), 3–11.
- Van der Marel, H.W., Beutelspacher, H., 1976. Atlas of Infrared Spectroscopy of Clay Minerals and Their Admixtures. Elsevier, Amsterdam.
- Van Huissteden, J., Kasse, C., 2001. Detection of rapid climate change in Last Glacial fluvial succession in The Netherlands. *Glob. Planet. Change* 28, 319–339.
- Van Steijn, H., Bertran, P., Francou, B., Héty, B., Texier, J.P., 1995. Models for the genetic and environmental interpretation of stratified slope deposits: review. *Permafrost. Periglac. Process.* 6, 125–146.
- Van Vliet-Lanoë, B., 1990. The genesis and age of the argillic horizon in Weichselian loess of Northwestern Europe. *Quat. Int.* 5, 49–56.
- Van Vliet-Lanoë, B., 2010. Frost action. In: *Stoops, G., Marcellino, V., Mees, F. (Eds.), Interpretation of Micromorphological Features of Soils and Regoliths*. Elsevier, The Netherlands, pp. 81–108.
- Wang, S.-L., Burr, G.S., Chen, Y.-G., Lin, Y., Wu, T.-S., 2013. Low-Temperature and temperature stepped-combustion of terrace sediments from Nanfu, Taiwan. *Radiocarbon* 55 (2–3), 553–562.
- Weiner, S., Bar-Yosef, O., 1990. States of preservation of bones from prehistoric sites in the Near East: a survey. *J. Archaeol. Sci.* 17, 187–196.
- Wetzel, R., 1958. Die Bocksteinschmiede mit dem Bocksteinloch, der Brandplatte und dem Abhang sowie der Bocksteingrotte. Teil 1. Veröffentlichungen aus der prähistorischen Abteilung des Ulmer Museums 1, Stuttgart.
- Wetzel, R., 1961. Der Hohlestein im Lonetal. Dokumente alteuropäischer Kulturen vom Eiszeitalter bis zur Völkerwanderung. Mitteilungen des Vereins für Naturwiss. und Math. Ulm (Donau) 27, 21–75.
- Wetzel, R., Bosinski, G., 1969. Die Bocksteinschmiede im Lonetal (Markung Rammingen, Kreis Ulm) I. Veröffentlichungen des Staatlichen Amtes für Denkmalpflege Stuttgart. Verlag Müller 6 Gräff, Stuttgart.
- Wilkerson, F.D., Schmid, G.L., 2003. Debris flows in glacier National park, Montana: geomorphology and hazards. *Geomorphology* 55 (1–4), 317–328.
- Wolff, W., 1962. Periglazial-Erscheinungen auf der Albhochfläche. Die Reprografie – Karl Mayer KG, Stuttgart.
- Yates, T.J.S., Spiro, B.F., Vita-Finzi, C., 2002. Stable isotope variability and the selection of terrestrial mollusc shell samples for ¹⁴C dating. *Quat. Int.* 87, 87–100.
- Yeshurun, R., Bar-Oz, G., Weinstein-Evron, M., 2007. Modern hunting behavior in the early middle paleolithic: faunal remains from Mishiya cave, Mount Carmel, Israel. *J. Hum. Evol.* 53, 656–677.